

E6^ΔE7, a Novel Splice Isoform Protein of Human Papillomavirus 16, Stabilizes Viral E6 and E7 Oncoproteins via HSP90 and GRP78

Masahiko Ajiro, Zhi-Ming Zheng

Tumor Virus RNA Biology Section, Gene Regulation and Chromosome Biology Laboratory, Center for Cancer Research, National Cancer Institute, National Institutes of Health, Frederick, Maryland, USA

ABSTRACT Transcripts of human papillomavirus 16 (HPV16) E6 and E7 oncogenes undergo alternative RNA splicing to produce multiple splice isoforms. However, the importance of these splice isoforms is poorly understood. Here we report a critical role of E6^ΔE7, a novel isoform containing the 41 N-terminal amino acid (aa) residues of E6 and the 38 C-terminal aa residues of E7, in the regulation of E6 and E7 stability. Through mass spectrometric analysis, we identified that HSP90 and GRP78, which are frequently upregulated in cervical cancer tissues, are two E6^ΔE7-interacting proteins responsible for the stability and function of E6^ΔE7, E6, and E7. Although GRP78 and HSP90 do not bind each other, GRP78, but not HSP90, interacts with E6 and E7. E6^ΔE7 protein, in addition to self-binding, interacts with E6 and E7 in the presence of GRP78 and HSP90, leading to the stabilization of E6 and E7 by prolonging the half-life of each protein. Knocking down E6^ΔE7 expression in HPV16-positive CaSki cells by a splice junction-specific small interfering RNA (siRNA) destabilizes E6 and E7 and prevents cell growth. The same is true for the cells with a GRP78 knockdown or in the presence of an HSP90 inhibitor. Moreover, mapping and alignment analyses for splicing elements in 36 alpha-HPVs (α -HPVs) suggest the possible expression of E6^ΔE7 mostly by other oncogenic or possibly oncogenic α -HPVs (HPV18, -30, -31, -39, -42, -45, -56, -59, -70, and -73). HPV18 E6^ΔE7 is detectable in HPV18-positive HeLa cells and HPV18-infected raft tissues. All together, our data indicate that viral E6^ΔE7 and cellular GRP78 or HSP90 might be novel targets for cervical cancer therapy.

IMPORTANCE HPV16 is the most prevalent HPV genotype, being responsible for 60% of invasive cervical cancer cases worldwide. What makes HPV16 so potent in the development of cervical cancer remains a mystery. We discovered in this study that, besides producing two well-known oncoproteins, E6 and E7, seen in other high-risk HPVs, HPV16 produces E6^ΔE7, a novel splice isoform of E6 and E7. E6^ΔE7, in addition to self-interacting, binds cellular chaperone proteins, HSP90 and GRP78, and viral E6 and E7 to increase the steady-state levels and half-lives of viral oncoproteins, leading to cell proliferation. The splicing *cis* elements in the regulation of HPV16 E6^ΔE7 production are highly conserved in 11 oncogenic or possibly oncogenic HPVs, and we confirmed the production of HPV18 E6^ΔE7 in HPV18-infected cells. This study provides new insight into the mechanism of splicing, the interplay between different products of the polycistronic viral message, and the role of the host chaperones as they function.

Received 3 October 2014 Accepted 30 December 2014 Published 17 February 2015

Citation Ajiro M, Zheng Z-M. 2015. E6^ΔE7, a novel splice isoform protein of human papillomavirus 16, stabilizes viral E6 and E7 oncoproteins via HSP90 and GRP78. *mBio* 6(1): e02068-14. doi:10.1128/mBio.02068-14.

Editor Michael J. Imperiale, University of Michigan

Copyright © 2015 Ajiro and Zheng. This is an open-access article distributed under the terms of the [Creative Commons Attribution-Noncommercial-ShareAlike 3.0 Unported license](https://creativecommons.org/licenses/by-nc-sa/4.0/), which permits unrestricted noncommercial use, distribution, and reproduction in any medium, provided the original author and source are credited.

Address correspondence to Zhi-Ming Zheng, zhengt@exchange.nih.gov.

This article is a direct contribution from a Fellow of the American Academy of Microbiology.

Human papillomaviruses (HPVs) are nonenveloped double-stranded DNA viruses which infect mucosal or skin keratinocytes. More than 120 HPV genotypes have been reported (1), and those responsible for malignant tumor formation are called high-risk or oncogenic HPVs, while those for benign anogenital warts are called low-risk or nononcogenic HPVs (2, 3). More than 95% of cervical cancers, 50 to 90% of other anogenital cancers, and 20 to 30% of oral and pharyngeal cancers are associated with persistent infection and host genomic integration of high-risk HPVs (3–5). Among the major genotypes of high-risk HPVs, namely, HPV16, -18, -31, -33, -45, and -58, HPV16 is the most prevalent genotype; it is responsible for ~60% of cervical cancer cases worldwide (4, 6).

Oncogenic activities of high-risk HPVs are mediated by two viral oncoproteins, E6 and E7. E6 and E7 oncoproteins target tumor suppressor proteins, such as p53 and pRB, to induce cell proliferation, antiapoptosis, genome instability, and escape from innate immune systems (7–9). In HPV16, these two viral oncogenes are transcribed from an early promoter, P₉₇, as a single E6E7 polycistronic pre-mRNA, and its transcriptional level and translational efficiency are regulated by an alternative RNA splicing machinery of host cells (7, 10, 11). This polycistronic pre-mRNA contains two introns and three exons, with intron 1 in the E6 open reading frame (ORF) containing three alternative 5' splice sites (ss) and three alternative 3' ss. Thus, alternative RNA splicing of this E6 intron produces multiple splice isoforms of the E6E7 RNA

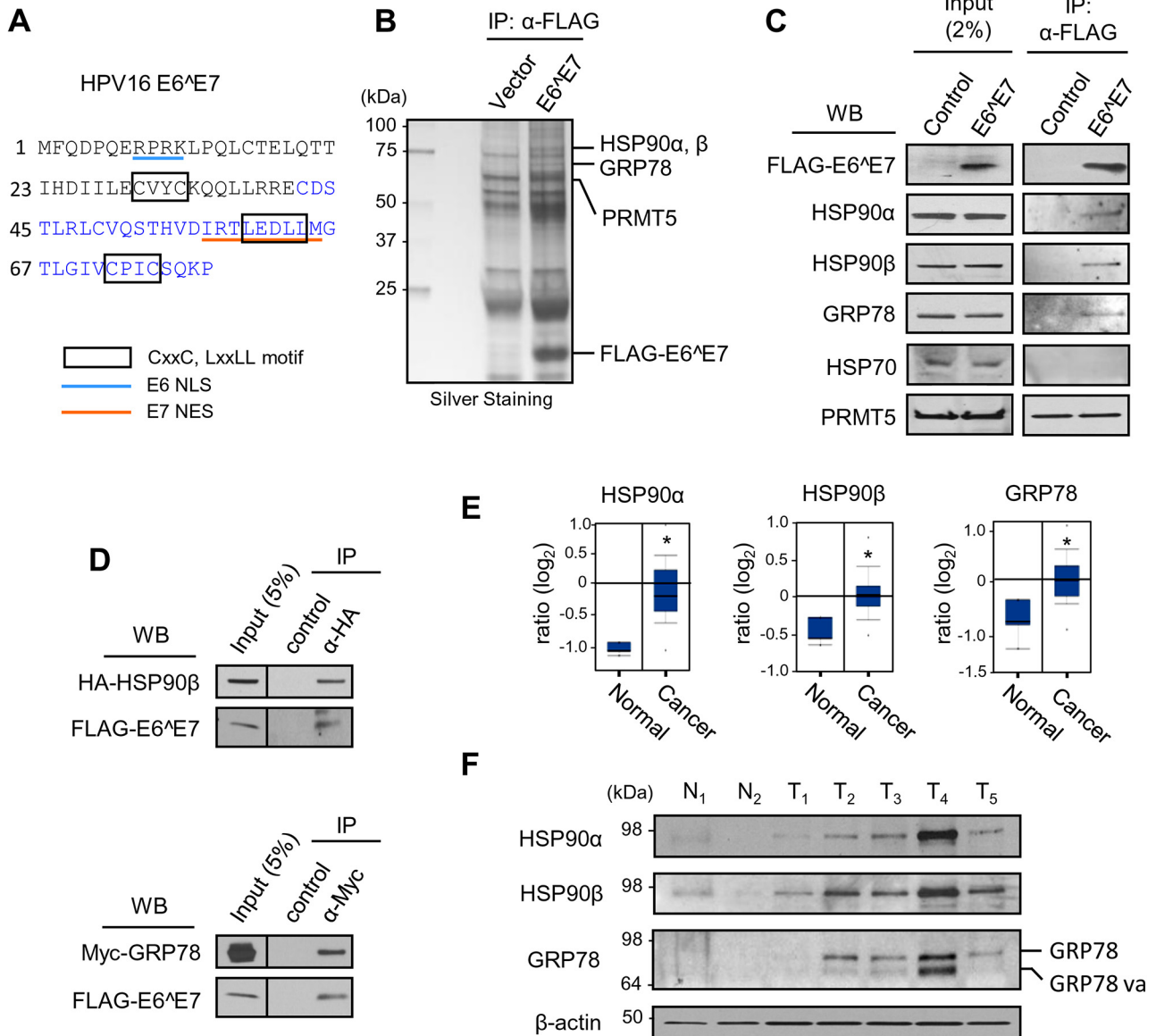


FIG 1 Coimmunoprecipitation (co-IP) and LC-MS/MS analysis identified HSP90 α , HSP90 β , and GRP78 as E6^{E7}-interacting proteins. (A) Diagram of HPV16 E6^{E7} amino acid residues. E6- and E7-derived amino acid residues are indicated in black and blue letters, respectively. The E6-derived nuclear localization signal (NLS) and E7-derived nuclear export signal (NES) are underlined. CXXC and LXXLL motifs are boxed. (B) Silver staining image of anti-FLAG-immunoprecipitated (α -FLAG) proteins from HEK293 cells transfected with a FLAG-E6^{E7} expression vector or an empty vector for 48 h. Proteins identified by LC-MS/MS are indicated on the right. (C and D) Western blot (WB) verification of the specific binding of endogenous HSP90 α , HSP90 β , and GRP78, but not HSP70 and PRMT5, to FLAG-E6^{E7} by anti-FLAG IP (C) or the binding of ectopic HA-HSP90 β or Myc-GRP78 to FLAG-E6^{E7} by anti-HA IP (D, top panel) or anti-Myc IP (D, lower panel). Cell lysate from an empty vector transfection served as an IP control in panel C, and Sepharose beads without antibody were used as an IP control in panel D. HEK293 cell lysates prepared at 48 h of transfection were used in all IP and Western blot assays. Western blotting was conducted with an antibody specific for an endogenous protein or a tag-specific antibody for an ectopic protein tag. (E) Relative mRNA levels of HSP90 α , HSP90 β , and GRP78 in normal cervix and cervical cancer tissues. *, $P < 1 \times 10^{-4}$ (Student's *t* test between two groups). Normal cervix specimens, $n = 5$; cervical cancer tissue specimens, $n = 40$. (F) Western blot analysis of HSP90 α , HSP90 β , GRP78, and GRP78va (a GRP78 splice isoform) (31) for normal cervix specimens (lanes N₁ and N₂) and cervical cancer tissues (lanes T₁, T₂, T₃, T₄, and T₅). β -actin was used as an internal loading control.

(12). E6^I and E6^{II} are two major splice isoforms of E6 and have been noticed for decades (13–15). E6^I RNA functions as an E7 mRNA for translation of E7 oncoprotein, while unspliced E6 RNA is responsible for full-length E6 expression (12, 16, 17). The role of E6^I protein in the regulation of cellular function and viral carcinogenesis remains under investigation (18–21).

E6^{E7} is another splice isoform produced by alternative splic-

ing from a 5' splice site at nucleotide (nt) 226 to a 3' splice site at nt 742 of the polycistronic E6E7 pre-mRNA (16, 22). This RNA splicing causes the N-terminal coding region of the E6 ORF to be spliced in frame with the C-terminal coding region of the E7 ORF. Thus, this spliced RNA isoform encodes an E6^{E7} fusion protein with a characteristic structure of the N-terminal half (41 aa residues) of E6 and the C-terminal half (38 aa residues) of E7 (Fig. 1A). E6^{E7}

was initially discovered through an *in vitro* splicing assay (16), and its existence was further confirmed in most HPV16-positive cervical cancer tissues and cell lines (12, 22). Although the consistent expression of E6^ΔE7 in HPV16-positive cell lines and cervical cancer tissues indicates that its potential function is to maintain tumor cell growth, its function has never been explored.

In this study, we report for the first time an important function of E6^ΔE7 in cervical carcinogenesis. E6^ΔE7 interacts with E6 or E7 and stabilizes E6 and E7 oncoproteins from proteasome-mediated degradation. The 90-kDa heat shock protein (HSP90) and 78-kDa glucose-regulated protein (GRP78) interact with E6^ΔE7 and cooperatively contribute to its function. Furthermore, we found that E6^ΔE7 is expressed not only in HPV16 but also in a subset of high-risk HPVs.

RESULTS

HSP90 α , HSP90 β , and GRP78 are HPV16 E6^ΔE7-interacting proteins. To uncover the function of E6^ΔE7, we first investigated proteins that interact with FLAG-tagged E6^ΔE7 (FLAG-E6^ΔE7) by anti-FLAG immunoprecipitation (IP) and nano-liquid chromatography–tandem mass spectrometry (LC-MS/MS). Bands of specific proteins pulled down by FLAG IP in FLAG-E6^ΔE7-expressing cells, compared with protein bands in control vector-transfected cells in a silver-stained gel, were analyzed by LC-MS/MS and subsequently identified as HSP90 α , HSP90 β , and GRP78 (Fig. 1B; see also Table S1 in the supplemental material). Co-IP and Western blotting confirmed the specific interactions of these three proteins with HPV16 E6^ΔE7 (Fig. 1C and D), while other proteins, including HSP70 and PRMT5, failed to be validated (Fig. 1C). HSP90 α , HSP90 β , and GRP78 are host chaperone proteins that regulate the stability of their specific client proteins by assisting their noncovalent folding and assembly. HSP90 α , HSP90 β , and GRP78 promote tumor progression by specifically targeting oncogenic proteins, such as HER2 (23), Raf-1 (24), and Akt (25), and are frequently up-regulated in most cervical cancer tissues (Fig. 1E and F) and other types of cancers (26, 27). E6^ΔE7 carries a nuclear localization signal (NLS) from the N-terminal half of E6 (28) and a nuclear export signal (NES) from the C-terminal half of E7 (29) (Fig. 1A). However, the majority of HPV16 E6^ΔE7 in transfected HEK293 cells is found in the cytoplasm, as has been seen for HSP90 and GRP78 (30–33), with a small fraction in the nucleus (see Fig. S1A in the supplemental material). Subsequent efforts failed to characterize E6^ΔE7 in destabilizing p53 and pRB or in preventing cell proliferation by overexpression in HPV-negative HEK293 or HCT116 cells (Fig. S1B and S1C).

HSP90 β and GRP78 promote the protein stability of HPV16 E6, E7, and E6^ΔE7, and E6^ΔE7 augments this function through protein-protein interactions. Given that HSP90 α , HSP90 β , and GRP78 are E6^ΔE7-interacting proteins, we speculated that these chaperone molecules may affect the steady-state level of E6^ΔE7. The levels of E6^ΔE7 protein and mRNA expression were examined in HEK293 cells with or without coexpression of HSP90 β or GRP78 from available expression vectors. Although the transfection efficiencies of the plasmids in these groups were similar as determined by neomycin phosphotransferase II (NPT II) expression from the neomycin resistance gene in the plasmid, we found an approximately >5-fold increase in the level of E6^ΔE7 protein, without a change of the E6^ΔE7 mRNA level, when coexpressed HSP90 β or GRP78 was ~40% or ~5-fold above its respective en-

dogenous level (Fig. 2A; see Fig. S2A in the supplemental material). Since E6^ΔE7 has the N-terminal half of E6 fused with the C-terminal half of E7, coexpression of HSP90 β or GRP78 was also examined in parallel for the steady-state levels of HPV16 E6 and E7 in HEK293 cells. Both HSP90 β and GRP78 were found to stabilize HPV16 E6 (Fig. 2B) and E7 (Fig. 2C) proteins but not their corresponding mRNAs. However, compared with GRP78 or HSP90 β , E6 appears to be a better responder to E6^ΔE7 than does E7 by transient expression assay. HSP90 β and GRP78 were also found to stabilize E6^{*}I protein, a truncated isoform of E6 (Fig. 2D). In either case, HSP90 β and GRP78 exhibited no effect on cellular β -actin protein and GAPDH mRNA (Fig. 2A to D).

Unexpectedly, the most drastic changes in the protein steady-state levels of E6 (~10-fold), E7 (~5-fold), and E6^{*}I (~10-fold) were found when they were coexpressed with E6^ΔE7 in the presence of endogenous HSP90 β and GRP78 in HEK293 cells (Fig. 2B to D). These changes were protein target specific because the coexpression of HSP90 β , GRP78, or E6^ΔE7 did not affect the level of green fluorescent protein (GFP) or mRNA (Fig. 2E) and could be reproducible with E7 in human primary foreskin keratinocytes (Fig. 2F) and HeLa cells (Fig. 2G). The effect of E6^ΔE7 on the E6 or E7 protein level in the cells could be greatly reduced when endogenous HSP90 was knocked down, resulting in a low level of E6^ΔE7 expression (Fig. 2H). Data suggest that E6^ΔE7 requires endogenous chaperones for its expression and activity. By using a proteasome inhibitor, MG132, we found that MG132 treatment of HEK293 cells for 6 h could increase HPV16 E6, E7, and E6^ΔE7 to comparable levels, as observed from E6^ΔE7 coexpression (Fig. 2I to K). The smaller size of an additional uncharacterized E6 band appeared in the presence of hemagglutinin (HA)-E6^ΔE7 but not in the presence of MG132 (Fig. 2I), suggesting its correlation with E6^ΔE7 expression.

Recent reports showed that proteins with acidic LXXLL motifs bind to and stabilize HPV16 E6 oncoprotein (34, 35) and that the hydrophobic surfaces and two CXXC zinc-binding motifs in HPV16 E7 are responsible for E7 homodimerization (36). Because those structures are retained in HPV16 E6^ΔE7 (Fig. 1A), we proposed that E6^ΔE7 might interact with E6 and E7. Indeed, E6^ΔE7 was found to bind both HPV16 E6 and E7 oncoproteins or vice versa by co-IP (Fig. 3A; see also Fig. S2B, left panel, in the supplemental material). Similarly, GRP78, which interacts with E6^ΔE7 (Fig. 1C and D), was capable of pulling down both E6 and E7 or vice versa by co-IP in the absence of E6^ΔE7 (Fig. 3B; see Fig. S2B, right panel, in the supplemental material). In contrast, HSP90 β , which also interacts with viral E6^ΔE7 (Fig. 1C and D), showed no binding activity to HPV16 E6 or E7 (Fig. 3C) nor to GRP78 (Fig. S2C), indicating that the effect of HSP90 β coexpression on the steady-state level of E6 or E7 is indirect.

The self-interaction of E6^ΔE7 was confirmed by co-IP of HA-E6^ΔE7 and FLAG-E6^ΔE7 (Fig. 3D). In addition, the coexpression of HA-E6^ΔE7 and FLAG-E6^ΔE7 was found to greatly increase the level of each protein, indicating that the self-interaction of E6^ΔE7 is important for its *in vivo* accumulation, as previously reported for HPV16 E6 and E7 (34, 37).

HPV16 E6^ΔE7 increases the half-lives of E6 and E7. To investigate how HPV16 E6^ΔE7 increases the steady-state level of E6 or E7 when coexpressed in HEK 293 cells, we transfected HEK293 cells with HPV16 E6 or E7 in the presence or absence of E6^ΔE7 and then treated the cells with cycloheximide (CHX) in a time course manner, followed by Western blotting of the cell lysates for

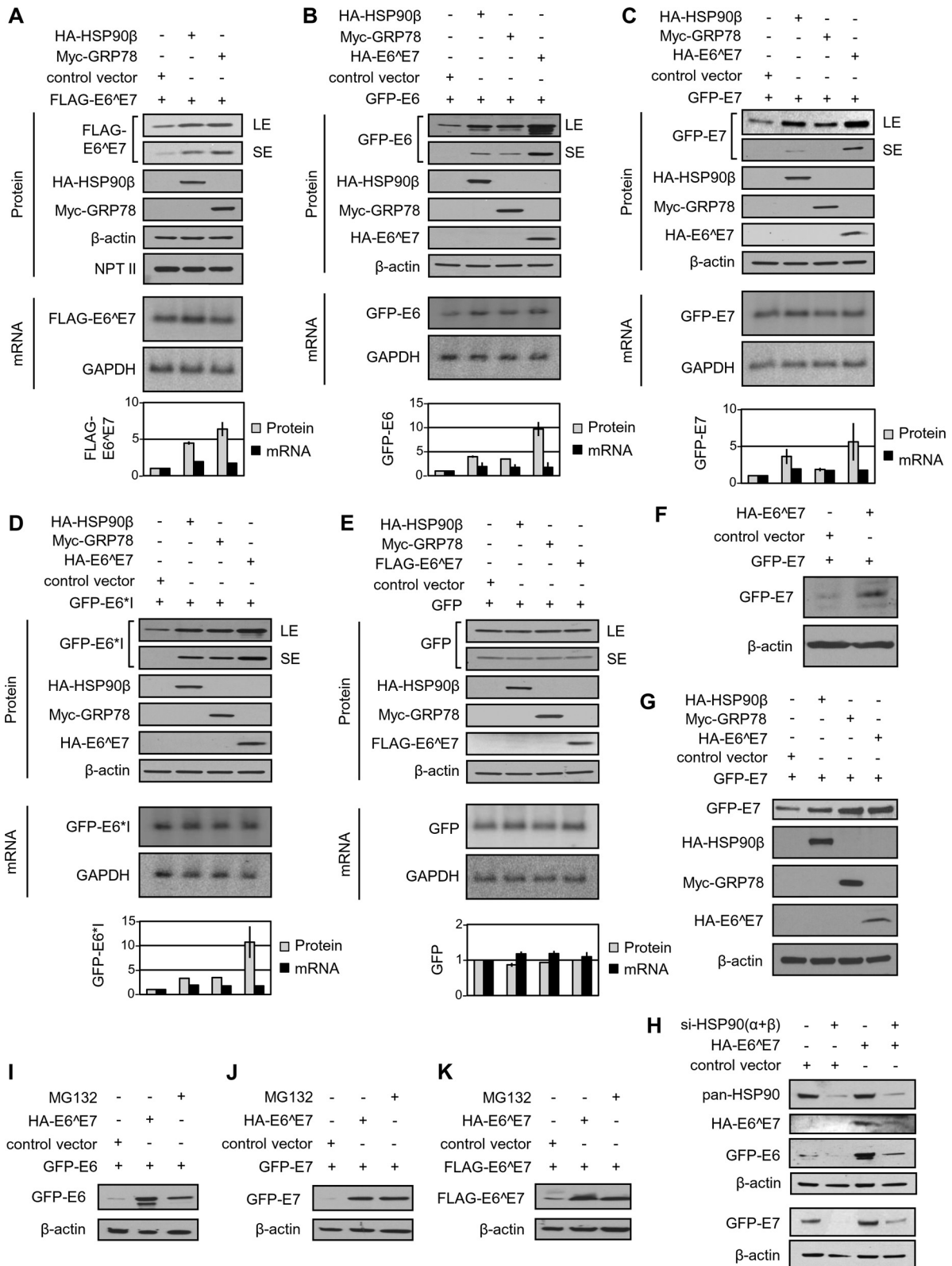


FIG 2 HPV16 E6^ΔE7, HSP90, and GRP78 promote the protein stability of HPV16 E6 and E7. (A to E) HSP90β and GRP78 increase the protein but not mRNA levels of HPV16 E6^ΔE7, E6, and E7 in HEK293 cells. Following cotransfection with the indicated vectors in each panel for 48 h, HEK293 cells were analyzed by Western blotting for protein expression levels of FLAG-E6^ΔE7 (A), GFP-E6 (B), GFP-E7 (C), GFP-E6*1 (D), or GFP (E) and by Northern blotting for the expression levels of corresponding mRNAs. An empty vector without any tagged protein expression served as a control for plasmid transfection and expression efficiency. LE, longer exposure; SE, shorter exposure. After normalization with β-actin in a Western blot or with GAPDH in a Northern blot, the relative (fold) changes in the levels of the

(Continued)

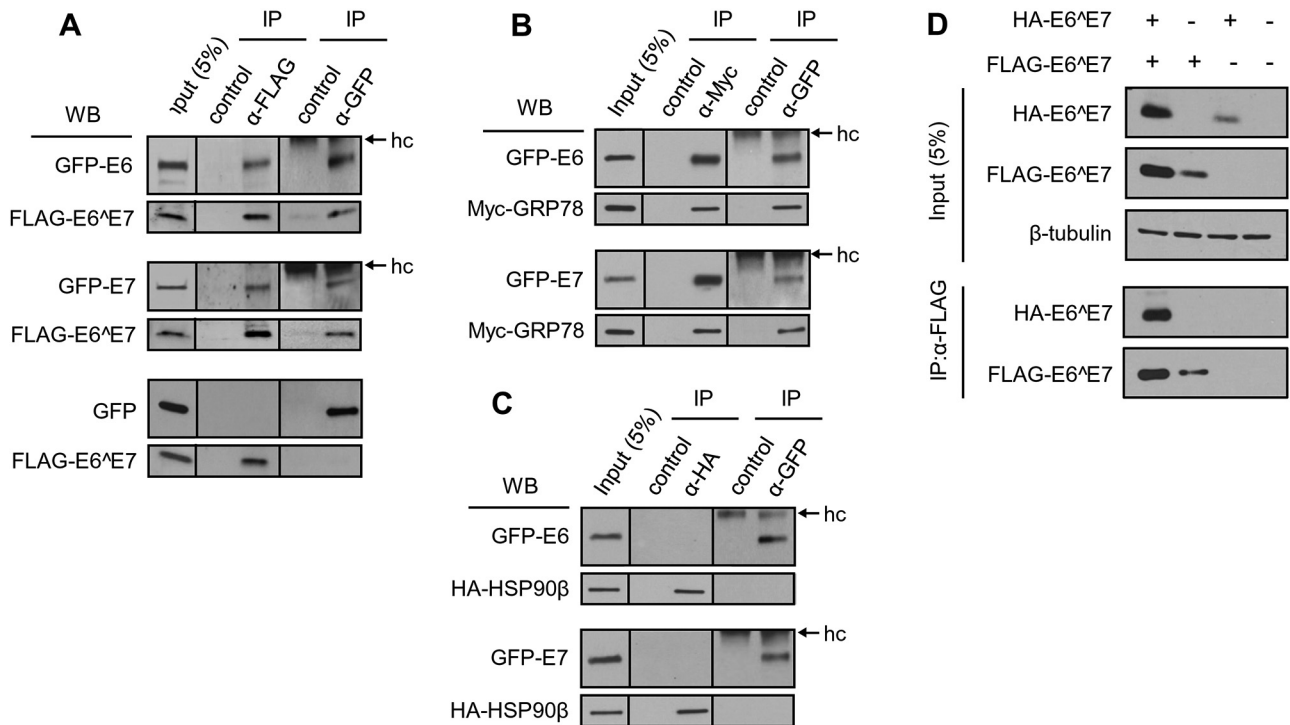


FIG 3 HPV16 E6 and E7 oncoproteins are proteins that interact with E6^{E7} and GRP78. (A to C) HPV16 E6 and E7 interact with E6^{E7} (A) and GRP78 (B), but not with HSP90β (C). HEK293 cells were transfected with FLAG-E6^{E7} (A), Myc-GRP78 (B), or HA-HSP90β (C) along with GFP-E6 or -E7 (A to C) for 48 h. The cell lysates were immunoprecipitated with the corresponding antibody, as indicated. Rabbit IgG was used as a negative control for each anti-GFP IP, and Sepharose beads without antibody served as controls for anti-FLAG, anti-HA, and anti-Myc IP. The interacting proteins in coimmunoprecipitations or in the input were examined by Western blotting (WB) with anti-GFP for GFP-E6 or -E7 (A to C), anti-FLAG for FLAG-E6^{E7} (A), anti-Myc for Myc-GRP78 (B), or anti-HA antibody for HA-HSP90β (C). hc, IgG heavy chain. (D) E6^{E7} is a self-interacting protein. HEK293 cells were cotransfected with a FLAG-E6^{E7} and an HA-E6^{E7} expression vector or an empty (-) control vector for 48 h. The cell lysates were blotted for the expression level of each protein (input panel) and immunoprecipitated with anti-FLAG antibody. The proteins pulled down by IP were blotted with an anti-FLAG antibody for FLAG-E6^{E7} or anti-HA antibody for HA-E6^{E7}. β-Tubulin served as a sample loading control.

E6 or E7 protein. CHX is an inhibitor of protein biosynthesis in eukaryotic organisms by blocking protein translational elongation (38), which enables us to compare the half-lives of E6 and E7 protein in the presence and absence of E6^{E7}. As shown in Fig. 4, the half-life of HPV16 E6 is ~45 min, and that of E7 is ~56 min. In these carefully controlled CHX experiments with NPT II as a transfection efficiency control and β-tubulin as a loading control for each sample, we found that E6^{E7} is capable of extending the half-life of E6 to ~119 min and that of E7 to ~154 min. These data indicate that E6^{E7} interacts with and stabilizes E6 or E7 protein.

HSP90β, GRP78, and E6^{E7} are required to maintain the steady-state level of E6 and E7 in HPV16-positive cervical cancer cells. We next looked into the functional regulation of E6 and E7 oncoproteins by endogenous HSP90β, GRP78, and E6^{E7} in HPV16-infected cervical cancer cells. We first applied 17-N-allylamino-17-demethoxygeldanamycin (17-AAG), an HSP90 ATPase inhibitor for both HSP90α and HSP90β that is in clinical trials for many types of cancer (27). In the presence of 17-AAG, HPV16-positive CaSki cells showed a decreased level of HPV16 E6 expression, with the increased stability of p53 indicative of E6 (17,

Figure Legend Continued

corresponding protein or mRNA in HEK293 cells cotransfected with HA-HSP90β, Myc-GRP78, or HA-E6^{E7} over the levels in cells transfected with an empty control vector are shown at the bottom of each panel in bar graphs. Error bars indicate standard deviations from two different blots. (F) E6^{E7} increases the E7 protein level in primary human foreskin keratinocytes. The keratinocytes were cotransfected with 4D-Nucleofector and GFP-E6 plus an HA-E6^{E7} expression vector or an empty control vector for 48 h and analyzed by Western blotting. (G) HA-HSP90β, Myc-GRP78, and HA-E6^{E7} increase GFP-E7 protein level in HeLa cells. HeLa cells were cotransfected with the indicated vectors for 48 h and analyzed by Western blotting. (H) The effect of HPV16 E6^{E7} on E6 and E7 stability relies on HSP90. HEK293 cells were transfected twice, with a 48-h interval, with siRNAs specific for HSP90α and -β isoforms or a nontargeting control siRNA (-) for 4 days. During the second siRNA transfection, the cells were cotransfected with an HA-E6^{E7} expression vector or a control vector (p3×FLAG-CMV14) in combination with a GFP-E6 or -E7 expression vector for 24 h and analyzed by Western blotting for HSP90α and -β knockdown efficiency with a pan-HSP90 antibody, E6^{E7} with an anti-HA antibody, or HPV16 E6 or E7 with an anti-GFP antibody. β-actin served as a loading control. (I to K) HA-E6^{E7} increased protein levels, and the levels of MG132-stabilized GFP-E6, GFP-E7, and FLAG-E6^{E7} are comparable in HEK293 cells at 48 h of transfection. The cell cotransfections were conducted with a GFP-E6 (I), GFP-E7 (J), or FLAG-E6^{E7} (K) expression vector along with an HA-E6^{E7} expression vector or control vector. For MG132 treatment, the cells transfected with a GFP-E6, GFP-E7, or FLAG-E6^{E7} expression vector were treated with MG132 (10 μM) or an equivalent amount of dimethyl sulfoxide (DMSO) 6 h prior to being harvested for Western blotting with an anti-GFP or anti-FLAG antibody. β-actin served as a sample loading control.

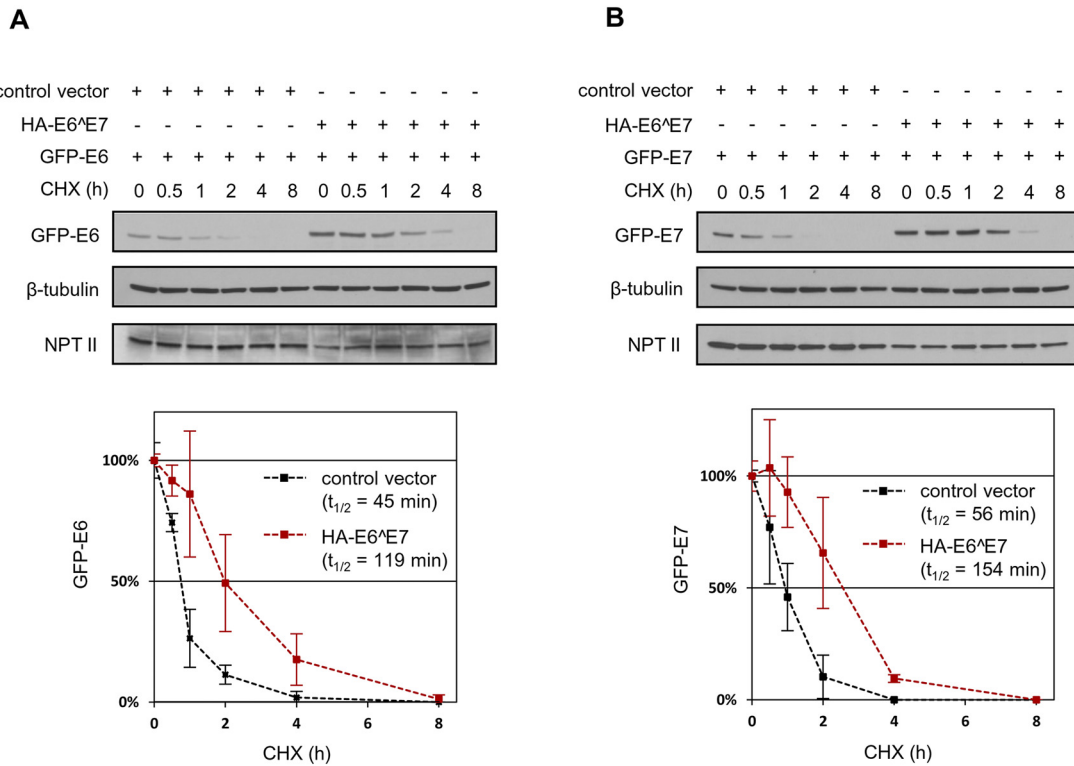


FIG 4 HPV16 E6^ΔE7 stabilizes E6 and E7 and prolongs the protein half-life. HEK293 cells were cotransfected with a GFP-E6 (A) or GFP-E7 (B) expression vector together with an HA-E6^ΔE7 or an empty control vector. After 16 h of cotransfection, the cells were treated with 0.1 mg/ml of cycloheximide (CHX) for the indicated times (0, 0.5, 1, 2, 4, and 8 h) before the sample collection for Western blotting with an anti-GFP antibody, anti-β-tubulin for sample loading, or anti-NPT II antibody for plasmid transfection efficiency. The half-life (t_{1/2}) of GFP-E6 or GFP-E7 was determined from a line plot analysis according to the following formulas, with its expression level at time zero being set to 100% and the two lines (x, y) crossing the 50% decay point (y = 0.5): for GFP-E6 with the control vector, y = -0.9583x + 1.2217; for GFP-E6 with HA-E6^ΔE7, y = -0.3683 + 1.2291; for GFP-E7 with the control vector, y = -0.6238x + 1.0828; and for GFP-E7 with HA-E6^ΔE7, y = -0.2802x + 1.2179, where x is the CHX treatment time (h) and y is the relative protein expression levels of GFP-E6 (A) or GFP-E7 (B). Black squares, protein expression level of GFP-E6 (A) or GFP-E7 (B) in HEK293 cells cotransfected with a control vector; red squares, protein expression level of GFP-E6 (A) or GFP-E7 (B) in HEK293 cells cotransfected with an HA-E6^ΔE7 expression vector.

39, 40) and E7 (Fig. 5A) reduction but with no change in the expression of full-length E6 (unspliced), E7 (E6*I), or E6^ΔE7 mRNA (Fig. 5B). This was expected because HSP90 and E6^ΔE7 together were found to stabilize viral E6 and E7 better than HSP90 or E6^ΔE7 alone (Fig. 2B and C), despite the finding that HSP90 itself does not interact with E6 or E7 (Fig. 3C). Consistently with the reduced expression of E6 and E7 oncoproteins, 17-AAG treatment blocked the growth of CaSki cells (Fig. 5C). GRP78 knock-down in CaSki cells also reduced the protein levels of both E6 (indicated by p53 increase) and E7 (Fig. 5D) and inhibited CaSki cell growth (Fig. 5E). All together, these data indicate that HSP90 and GRP78 are two chaperone proteins important for maintaining the steady-state levels of viral E6 and E7 oncoproteins for their oncogenic properties.

Functional regulation of HPV16 E6 and E7 oncoproteins by E6^ΔE7 was investigated by specific knockdown of E6^ΔE7 expression, although it is difficult for us to detect the E6^ΔE7 protein as well as the E6, E6*I, and E6*II proteins in cervical cancer cell lines (see Fig. S3 in the supplemental material). We designed a small interfering RNA (siRNA) targeting to the splice junction region covering the nt 226 5' ss and nt 742 3' ss (si-E6^ΔE7) (Fig. 5F) to knock down E6^ΔE7 expression in HPV16-positive CaSki cells. We found that this si-E6^ΔE7 exhibited a high efficiency and specificity in knocking down E6^ΔE7 RNA (nt 226 to 742) in CaSki cells,

without affecting full-length E6 RNA (unspliced), other alternatively spliced isoform RNAs, such as E6*I and E6*II, from HPV16 early transcripts, or cellular GAPDH (glyceraldehyde-3-phosphate dehydrogenase) RNA (Fig. 5G). Western blotting showed that the protein levels of both E6 and E7 in CaSki cells were decreased by the knockdown of E6^ΔE7 (Fig. 5H, where E6's decrease is indicated by p53's increase), resulting in cell proliferation retardation (Fig. 5I). Data suggest that the expression of E6^ΔE7 is important for the steady-state levels of both E6 and E7 oncoproteins in CaSki cells. This assumption was further validated by overexpression of E6^ΔE7 in CaSki cells, where E7 oncoprotein could be stabilized upon E6^ΔE7 overexpression, leading to a decrease in pRB protein level and an increase in CaSki cell proliferation (Fig. 5J and K). E6^ΔE7 overexpression displayed no effect on the growth of C33A cells, a cervical cancer cell line without HPV infection (Fig. 5L and M) but carrying mutant p53 and pRB (41).

Conservation of E6^ΔE7 among other high-risk HPVs. We next investigated alternative RNA splicing to produce E6^ΔE7 RNA from polycistronic early pre-mRNAs of other high-risk HPVs. The first step of RNA splicing by the cellular splicing machinery is to recognize a branch point sequence (BPS) and a polypyrimidine tract upstream of a 3' ss, respectively, by SF1 and U2AF65, and of a 5' ss by snRNP U1, followed by the stable association of U2

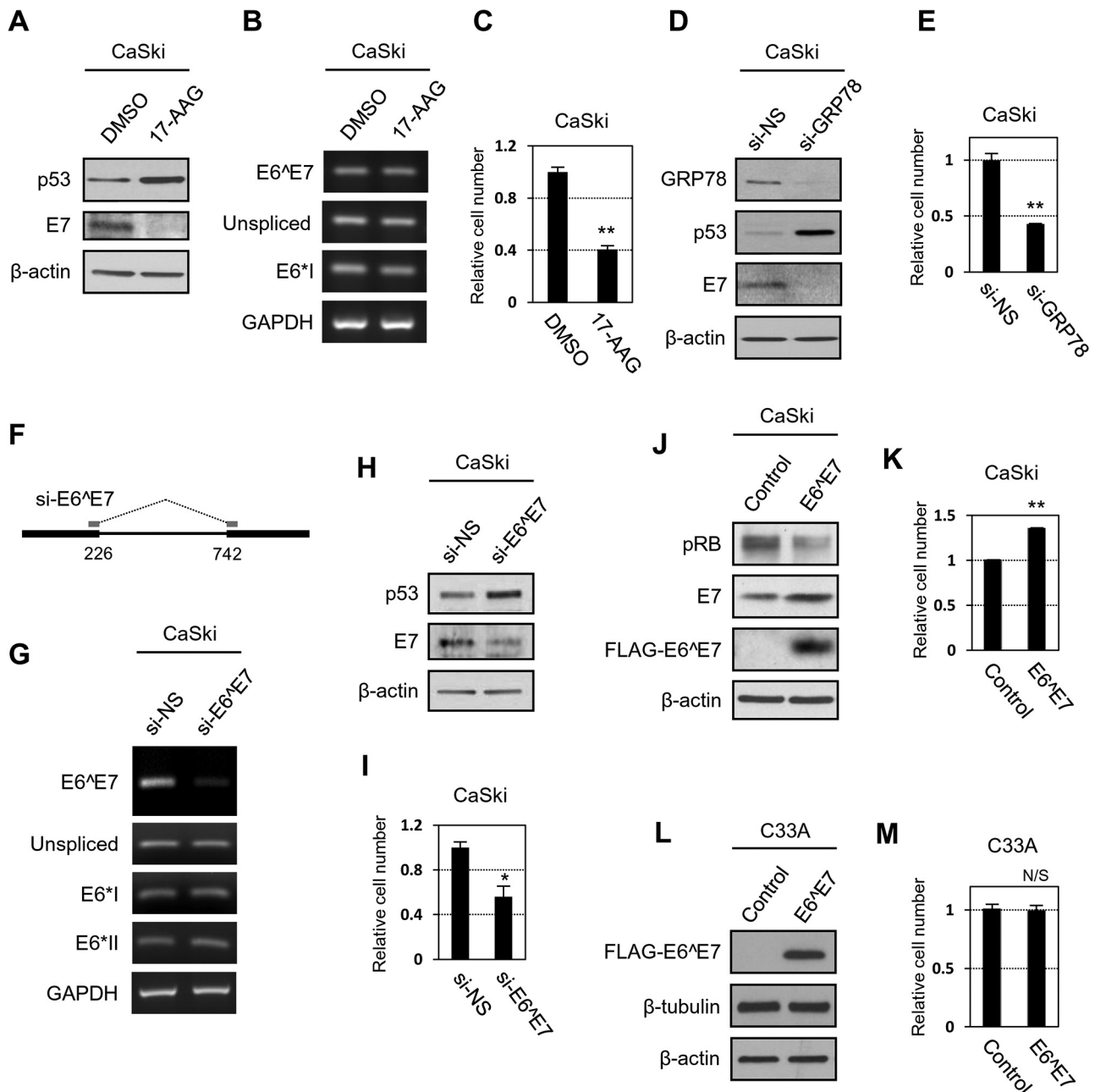


FIG 5 HSP90, GRP78, and E6^ΔE7 are required to maintain a steady-state level of E6 and E7 in HPV16-positive CaSki cells. (A to C) A functional HSP90 is required for the stability of HPV16 E6 and E7 and proliferation of cervical cancer cells. HPV16-positive CaSki cells treated with 5 μ M 17-AAG or DMSO for 48 h were examined by Western blotting (A), RT-PCR (B), and a cell proliferation assay (C). p53 was used to indicate E6. GAPDH served as a loading control in RT-PCR. (D and E) Knockdown of GRP78 expression in CaSki cells destabilizes E6 and E7 and inhibits cell growth. CaSki cells treated twice with 40 nM nontargeting siRNA (si-NS) or GRP78 siRNA (si-GRP78) for 96 h were examined by Western blotting (D) and a cell proliferation assay (E). (F to I) Knockdown of E6^ΔE7 expression in CaSki cells destabilizes viral E6 and E7 and prevents cell growth. An E6^ΔE7-specific siRNA (si-E6^ΔE7) for the nt 226-to-nt 742 splice junction (F) was designed to silence E6^ΔE7 expression without affecting other E6 splice isoform RNAs, as shown by RT-PCR (G). CaSki cells transfected twice with 40 nM si-NS or si-E6^ΔE7 at 48-h intervals for 96 h were examined for E6 (p53) and E7 expression (H) and cell proliferation (I). See the details in panels A to C. (J and K) Overexpression of E6^ΔE7 in CaSki cells increases E7 stability (J) and promotes cell proliferation (K). CaSki cells were transfected twice (for Western blotting at day 5) or three times (for cell proliferation at day 7) with a FLAG-E6^ΔE7 or an empty vector at 24-h intervals. (L and M) Overexpression of E6^ΔE7 has no effect on C33A, an HPV-negative cervical cancer cell line containing mutations in both p53 and pRB. C33A cells transfected with a FLAG-E6^ΔE7 or an empty vector as described for panels J and K served as a cell line control to CaSki cells, and results were analyzed by Western blotting (L) and a cell proliferation assay (M) at days 5 and 7, respectively. *, $P < 0.05$; **, $P < 0.01$. Nonsignificance (N/S), $P \geq 0.05$ by Student's t test (C and E, I and K, and M). (A, D, H, J, and L) β -Actin served as a sample loading control.

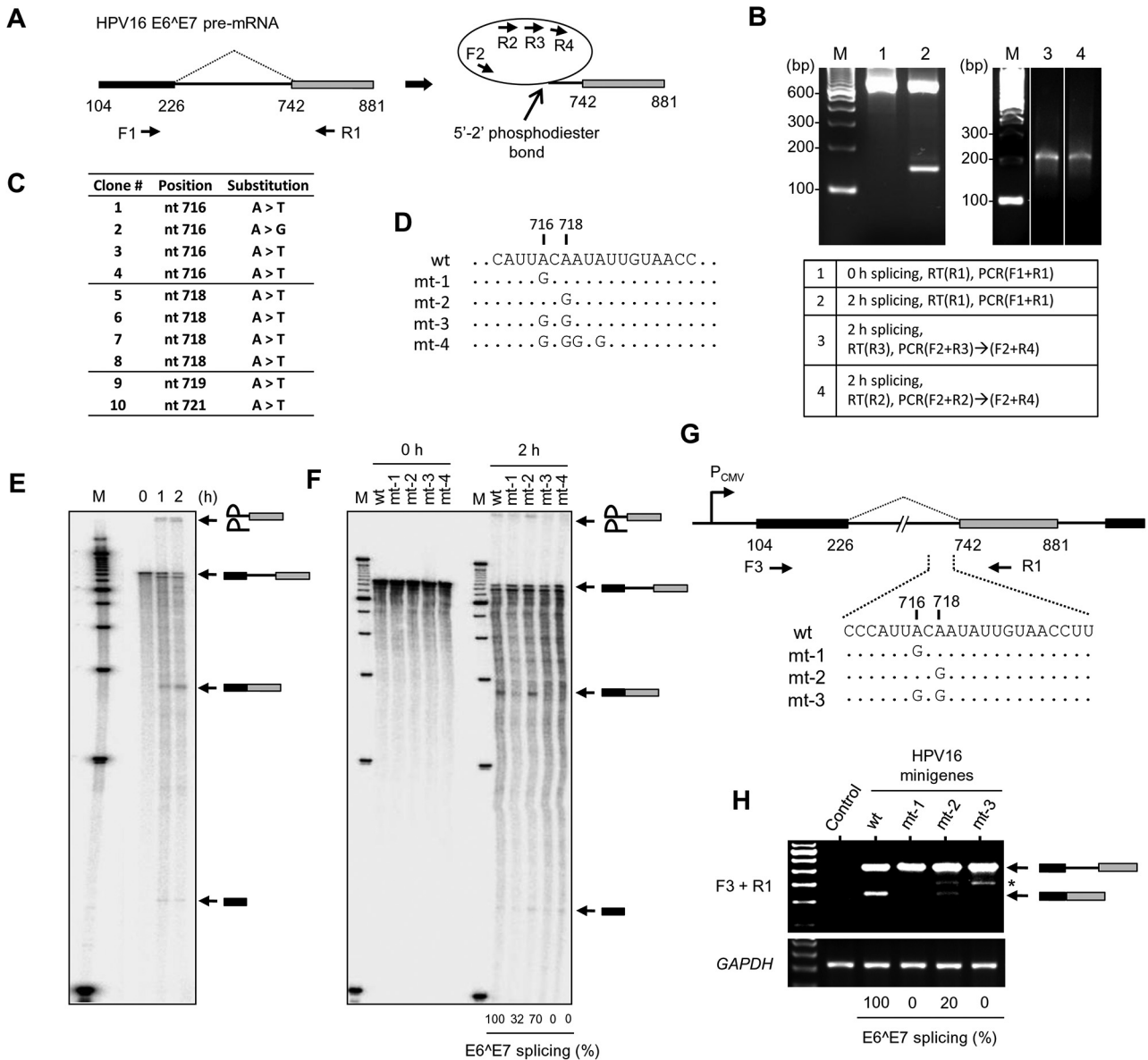


FIG 6 Mapping of RNA *cis* elements for splicing of HPV16 E6^ΔE7 pre-mRNA. (A) Diagram of a lariat RT-PCR strategy to map the BPS responsible for splicing of E6^ΔE7 pre-mRNA, with the indicated primers (F1 to F2 and R1 to R4). (B) Validation of *in vitro* splicing (2 h) of E6^ΔE7 pre-mRNA by RT-PCR. The left panel indicates the fully spliced products at a size of 136 nt. The right panel indicates the products of lariat RT-PCR at a size of ~200 nt. Combinations of primers used in RT-PCR are indicated in the box below. Lane M, molecular size markers. (C) Summary of the mapped branch sites by lariat RT-PCR. (D) Introduction of the A-to-G mutation (mt-1, mt-2, mt-3, and mt-4) into the mapped branch sites for *in vitro* RNA splicing. Nucleotides identical to the wild-type (wt) nucleotide are indicated by dots. (E) Reconstitution of E6^ΔE7 RNA splicing *in vitro*. Following the splicing reaction in HeLa cell nuclear extract for the indicated times (h), the spliced products were analyzed in a 6% polyacrylamide gel with 7.5 M urea. Identities of each band are indicated on the right. (F) E6^ΔE7 pre-mRNAs with wt or mutant branch sites were used for a 2-h reaction of *in vitro* splicing. Relative E6^ΔE7 splicing efficiencies (percentages) were calculated as described previously (12) and are indicated in the bottom. The identities of each band are indicated at the right. (G) Diagram of the minigene vectors to express E6^ΔE7 pre-mRNAs with a wt or mutant branch site (mt-1, mt-2, or mt-3). (H) RT-PCR was performed on total RNA of HEK293 cells transfected with E6^ΔE7 minigenes or a control vector for 24 h to detect unspliced and spliced E6^ΔE7 mRNAs (for the upper panel, primers F3 and R1 were used). GAPDH served as a loading control (lower panel). The identity of each band is indicated at the right. *, a nonspecific amplicon. Relative E6^ΔE7 splicing efficiencies (percentages) are indicated at the bottom.

snRNP to the BPS to proceed to catalytic steps (42, 43). Although the production of the HPV16 E6^ΔE7 splice isoform takes place from a 5' ss at nt 226 to a 3' ss at nt 742, the BPS governing the first step of splicing was unknown. By using a lariat reverse transcription (RT)-PCR technique in the presence of SuperScript II reverse transcriptase, we were able to amplify a splicing intermediate lariat structure in which the 5' phosphate of the guanosine at the 5' end

of the intron is linked to the 2' hydroxyl group of the adenosine at the BPS branch site (BS) to form a 5'-to-2' phosphodiester linkage (44, 45) (Fig. 6A). Since this 5'-2' link makes the lariat in a circular form and the SuperScript II reverse transcriptase may read through the 5'-2' phosphodiester bond, two paired primers in opposite directions designed to detect the lariats would be able to amplify a product running through the link with a nucleotide

substitution at the branch site (Fig. 6A, right panel). This was achieved by using HeLa nuclear extract for *in vitro* RNA splicing of HPV16 E6^ΔE7 RNA (Fig. 6B, left panel) and then lariat RT-PCR of the *in vitro*-spliced products (Fig. 6B, right panel). Gel purification, cloning, and sequencing of the single nested-PCR product (Fig. 6B, right panel) identified two adenosines, one at nt 716 (4/10 clones) and the other at nt 718 (4/10 clones); these are two major alternative branch site adenosines for splicing of the HPV16 E6^ΔE7 RNA. We also found that an adenosine either at nt 719 or at nt 721 might serve as a minor site (Fig. 6C; see Fig. S4 in the supplemental material).

Subsequently, we introduced point mutations (A→G) at these positions (Fig. 6D) and compared their effects on the *in vitro* splicing of ³²P-labeled HPV16 E6^ΔE7 pre-mRNA (Fig. 6E). As shown in Fig. 6F, an A-to-G mutation at nt 716 (lanes mt-1) suppressed the splicing efficiency of E6^ΔE7 pre-mRNA by 68%, but introduction of the same mutation at nt 718 reduced the splicing efficiency by only 30% (lanes mt-2). However, simultaneous introduction of the A-to-G mutation at both nt 716 and nt 718 (lanes mt-3) or together with the A-to-G mutations at nt 719 and nt 721 (lanes mt-4) completely blocked the *in vitro* splicing of E6^ΔE7 pre-mRNA. Based on these observations, we conclude that splicing of HPV16 E6^ΔE7 pre-mRNA takes place by use of two alternative branch sites, of which nt 716A serves as a major site and nt 718A serves as a minor site. The same results were also seen by *in vivo* splicing assays in HEK293 cells transfected with an HPV16 E6^ΔE7 minigene (Fig. 6G and H). We further confirmed that the A-to-G mutation at nt 716 (lanes mt-1) completely abrogated E6^ΔE7 splicing in HEK293 cells but that the same mutation at nt 718 (lanes mt-2), although it also reduced splicing greatly, retained 20% of the splicing efficiency of the wild-type (wt) construct (Fig. 6H). As expected, a combination of both mutations in the two mapped branch site adenosines of the HPV16 E6^ΔE7 minigene (mt-3) were detrimental to *in vivo* E6^ΔE7 splicing (Fig. 6H).

To date, HPV16, among all known HPVs, appears to be the only genotype to express E6^ΔE7. However, we found that the E6^ΔE7-splicing *cis* elements (5' ss, BS, polypyrimidine tract, and 3' ss) identified in HPV16 are highly conserved among 11 of 36 α -HPVs (13 from high-risk, 4 from possibly high-risk, 8 from low-risk, and 11 from risk-undetermined HPVs), of which 8 are high-risk HPVs (HPV16, -18, -31, -39, -45, -56, -59, and -73), 1 is possibly a high-risk HPV (HPV30), and 2 are low-risk HPVs (HPV42 and HPV70) (Fig. S5A and S6). Interestingly, this alignment analysis also showed that HPV30, -42, and -70, like HPV16 and HPV18, contain an intron in the E6 ORF (Fig. S5B), which is characteristic of high-risk, but not of low-risk, HPVs (7). The other remaining HPVs analyzed, including high-risk HPV33, -35, -51, -52, and -58 (46), appear to lack either a 5' ss, a 3' ss, or a visible BS for E6^ΔE7 splicing in the corresponding regions of HPV16, indicating that they express no E6^ΔE7 (Fig. S5A). In the HPVs with the conserved E6^ΔE7-splicing *cis* elements, the N-terminal half of the E6 ORF could hypothetically be spliced in frame into the C-terminal half of the E7 ORF, as seen in HPV16 (Fig. S6). Based on these analyses, we examined and confirmed by RT-PCR the expression of HPV18 E6^ΔE7 in HPV18-positive HeLa cells but not in HEK293 cells or in HPV16-positive CaSki cells (Fig. 7A and B). Cloning and sequencing of the RT-PCR products further revealed that HPV18 E6^ΔE7 is a splicing product from nt 233 to nt 791 (Fig. 7C). In addition to its expression in cervical cancer cell lines, E6^ΔE7 expression from raft tissues with

productive HPV16 or HPV18 infection (47) could be verified by RT-PCR (Fig. 7D). However, we were unable to detect HPV18 E6^ΔE7 protein by using an antibody against the HPV18 E6 N terminus that recognizes ectopically expressed HPV18 E6 but not E6**I* in HEK293 cells or native HPV18 E6 and E6**I* from HPV18-infected raft tissues or HeLa cells.

Quantification of E6 and its splice variants E6**I*, E6**II*, and E6^ΔE7 in HPV16-positive cervical cancer cell lines and tissues.

The HPV16 early pre-mRNA derived from its early promoter P₉₇ is a polycistronic transcript bearing two introns and three exons. In HPV16-infected cells, this viral pre-mRNA undergoes extensive alternative RNA splicing in order to express other viral ORFs downstream. One of the two introns is positioned in the E6 ORF and contains three alternative 5' ss (nt 191, 221, and 226) and three alternative 3' ss (nt 409, 526, and 742). Although the nt 226 5' ss and the nt 409 3' ss are two splice sites preferentially selected over the other splice sites, crossing over the intron to excise a minimal length of the intron in RNA splicing (12), splicing of the intron in the E6 ORF will disrupt the integrity of the E6 ORF and prevent the expression of full-length E6 protein. Thus, we quantified the relative usage of E6^ΔE7 over that of unspliced E6 and two other well-described E6 splice isoforms, E6**I* derived from splicing the nt 226 5' ss to the nt 409 3' ss and E6**II* derived from splicing the nt 226 5' ss to the nt 526 3' ss, in HPV16-positive cervical cancer cells and cervical cancer tissues by splicing junction-specific TaqMan real-time RT-PCR (Fig. S7). As shown in Tables 1 and S2, we found that the copy number of HPV16 E6^ΔE7 mRNA, as with E6, E6**I*, and E6**II*, varies from one cell line or tumor tissue to another and that its proportion is much lower (0.2% to 18.4%) than those of the unspliced, full-length E6 RNA (13.2% to 55.9%), E6**I* (29.5% to 79.9%), and E6**II* (4.6% to 34.6%) in the examined cervical cancer cell lines or tissues.

DISCUSSION

In this study, we showed a crucial role of HPV16 E6^ΔE7 in stabilizing E6 and E7 oncoproteins and evidenced its contribution to oncogenicity in cooperation with E6 and E7, although E6^ΔE7 itself does not independently affect the stability of p53 or pRB. Our data also revealed that the stability of E6^ΔE7, E6, and E7 requires HSP90 and GRP78, two host chaperones frequently overexpressed in cancer cells. E6^ΔE7 interacts with GRP78, HSP90, and HPV16 E6 and E7. GRP78, but not HSP90 β , interacts with E6 and E7. We found that the role of E6^ΔE7 appears critical in stabilizing E6 and E7, with E6 being a better responder than GRP78 or HSP90 β by transient expression. However, the E6^ΔE7 enhancement of E6 or E7 stability becomes minimal in cells with a reduced expression of GRP78 or HSP90, where E6^ΔE7 itself is unstable. We could not see greater loss of the protein stability when both chaperones were knocked down or inhibited. Instead, inhibition or knockdown of HSP90 increases the expression of GRP78 (48, 49). Because HSP90 does not interact with E6, E7, or GRP78, the effect of HSP90 on E6 and E7 stability must be exerted through other cofactors. In general, HSP90 collaborates with a large set of co-chaperones in assembling a functional chaperone machinery to assist in client protein folding to the native state (50). Other chaperone proteins (HSP70, HSP40, and cyclophilin) in the regulation of HPV entry and genome replication have been reported in HPV11 (51), HPV16 (52), and HPV31 (53).

It is known that E6 and E7 are unstable unless they are associated with appropriate proteins. Recent studies indicated that E6

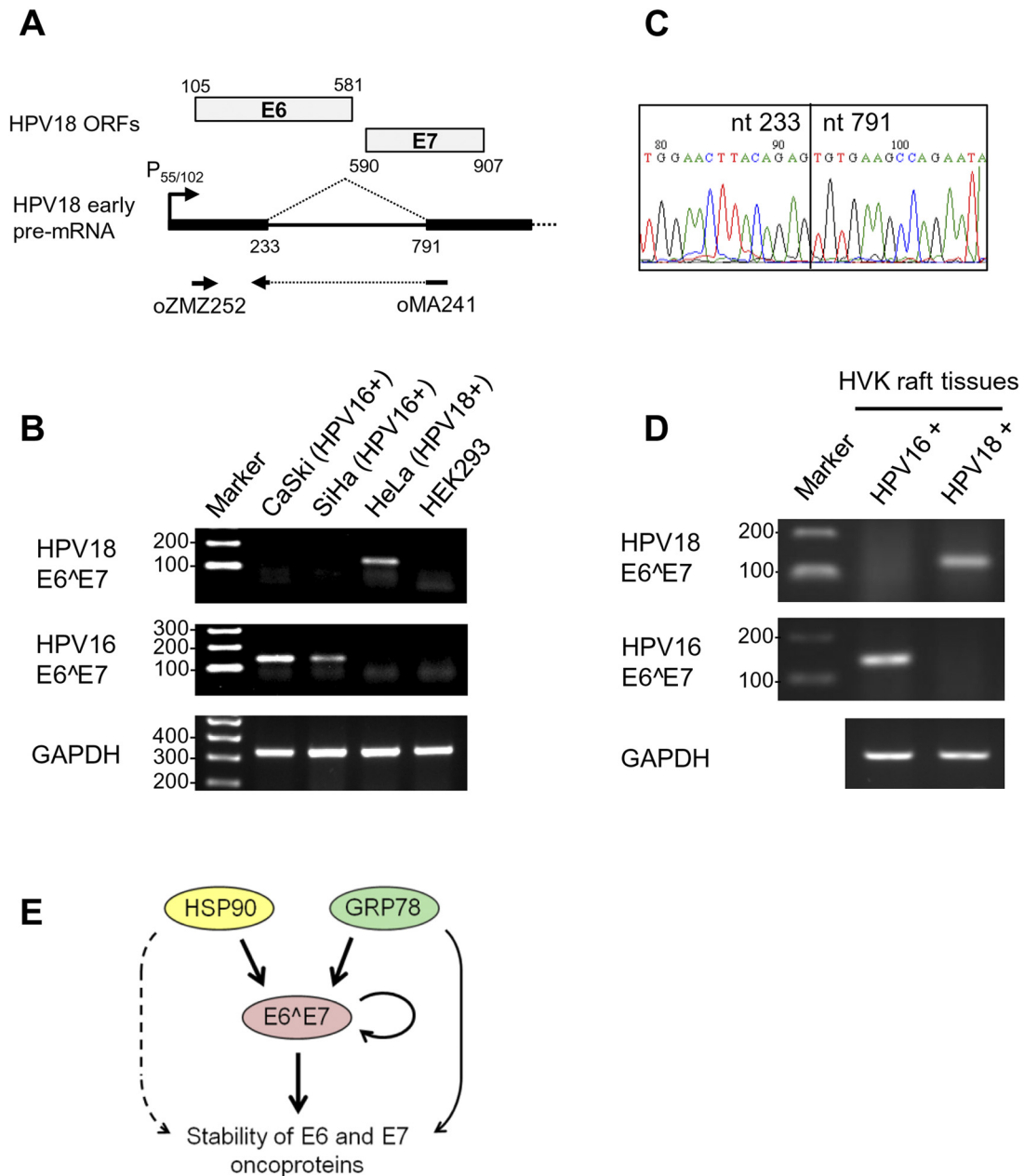


FIG 7 Expression of HPV18 E6[^]E7 in an HPV18-infected cell line and raft tissues. (A) Diagram of alternative RNA splicing from the nt 233 5' ss to the nt 791 3' ss to produce E6[^]E7 mRNA from HPV18 early transcripts. The ORFs of the HPV18 E6 and E7 oncogenes are indicated at the top. Primers specific for HPV18 E6[^]E7 mRNA detection by RT-PCR are indicated below the pre-mRNA. (B) Detection of HPV18 E6[^]E7 from HPV18-positive HeLa cells and HPV16 E6[^]E7 from HPV16-positive CaSki or SiHa cells by RT-PCR. HPV-negative HEK293 cells and GAPDH mRNA served as controls. (C) Determination of the HPV18 E6[^]E7 splice junction by sequencing of RT-PCR products gel purified from the experiment whose results are shown in panel B. (D) Detection of HPV18 E6[^]E7 and HPV16 E6[^]E7 in the HVK raft tissues with the corresponding virus infection. (E) E6[^]E7 plays a central role in HSP90 and GRP78 regulation of HPV16 E6 and E7 protein stability through protein-protein interactions. HSP90 and GRP78 are also involved in the stability of HPV16 E6 and E7, either indirectly (dashed arrow) or directly (solid arrow).

can be stabilized by heterodimerization with E6-AP through an acidic LXXLL motif (34). Other studies also suggested that both E6 and E7 may be stabilized through homodimerization in biochemical assays, which are mediated by two separated CXXC zinc-binding motifs within E6 and E7 proteins (36, 37, 54). Although HPV16 E6[^]E7, which retains two zinc-binding motifs, interacts with both HPV16 E6 and E7, how this protein-protein interaction

contributes to stabilize E6 and E7 remains unknown. By interaction with E6 or E7, E6[^]E7 perhaps serves as a bridge to recruit HSP90 for better assembly of a functional chaperone machinery to facilitate E6 or E7 folding. Alternatively, E6[^]E7, by interaction with HSP90 and GRP78, may simply serve as a cofactor to promote chaperone activities, as reported for other HSP90 cofactors (50). Why both chaperone proteins are required for stabilization

to occur remains to be understood. One possibility is that they are required for the different transitional states of the newly synthesized protein. Nevertheless, our study indicates that E6^ΔE7 plays a central role in HSP90's and GRP78's regulation of the stability of E6 and E7 (Fig. 7E). Since HSP90 and GRP78 also stabilize E6^ΔE7, this study provides the further evidence of a positive-feedback loop in infected cells to promote the steady-state levels of E6 and E7 oncoproteins.

Early studies of bovine papillomavirus 1 (BPV-1)-transformed mouse C127 cells showed that the BPV-1 E6 ORF could be spliced to the E7 ORF in frame, leading to the production of a novel E6^ΔE7 mRNA to encode a hypothetical E6^ΔE7 fusion protein with a size of 183 aa residues (71 aa residues from E6 and 112 aa residues from E7) (55, 56). Subsequent investigation of a cDNA derived from the E6^ΔE7 mRNA showed no transformation activity in mouse C127 cells (56). Although the in-frame RNA splicing of the E6 ORF to the E7 ORF was identified in HPV16 in 2004 (16, 22), whether such a splicing event exists in other oncogenic HPVs was unknown, and its regulation by RNA *cis* elements was poorly understood. In this report, we mapped the branch point and polypyrimidine tract for the selection of the nt 742 3' ss to produce E6^ΔE7 mRNA and successfully identified the nt 716 and nt 718 adenosines as two alternative branch sites in the BPS to guide the usage of this 3' ss. Subsequent clustering analysis revealed the conservation of these RNA *cis* elements from early HPV16 to HPV18, -30, -31, -39, -42, -45, -56, -59, -70, and -73 transcripts (Fig. S5). We confirmed this production of E6^ΔE7 in HPV18-infected cells and cervical cancer cell lines by RT-PCR. HPV42 and HPV70 are two low-risk HPVs but could be detected in cervical intraepithelial neoplasia (CIN) lesions and anogenital cancer (57–61). Our analysis indicates that both HPV42 and HPV70 contain an E6 intron leading to production of E6**I*, a characteristic of high-risk HPVs (7). Thus, the presence of viral E6^ΔE7 in HPV16, HPV18, or other high-risk HPV infection to stabilize viral E6 and E7 might provide oncogenic advantages to these HPVs over the other HPVs lacking E6^ΔE7 expression in cervical-lesion progression.

An intriguing question in this study is how a low level of E6^ΔE7 transcripts relative to E6- and E7-encoding transcripts could translate a sufficient level of protein to alter the level of E6 or E7 protein. Both E6 and E7 have very short half-lives of less than 60 min, but in the presence of viral E6^ΔE7, these proteins' half-lives may be increased to ~120 min for E6 and ~150 min for E7 (Fig. 4), indicating that the viral E6^ΔE7 functions as a potent protein to promote the stability of E6 and E7. We confirmed this in HPV16-positive CaSki cells in which the expression of E6^ΔE7, despite being at protein level undetectable by Western blotting with antibodies against HPV16 E6 (Fig. S3), is important for the stability of E6 and E7, because siRNA knockdown of E6^ΔE7 expression in CaSki cells may trigger the instability of both E6 and E7 (Fig. 5). HPV16 E6 is another protein notorious for its difficulty of detection in HPV16-positive cell lines (Fig. S3), but it is very potent in the induction of p53 degradation (17, 39). Together, our data indicate that a potent protein may function well at a very low level and thus does not need to be highly expressed.

Although therapeutic vaccines specifically targeting oncogenic E6 or E7 have been under development (62–64), the current treatment of cervical cancer is dependent on surgical procedures and conventional chemoradiotherapy. The major difficulty of targeting E6 and E7 is that E6 and E7 oncogenic activities are mediated

through protein-protein interactions rather than enzymatic activities. Inhibition of E6 and E7 expression through siRNA or small peptides appeared effective *in vitro*, but these efforts were not designed for *in vivo* preclinical trials, and the siRNA or small peptides are difficult to deliver (17, 65, 66). However, our findings in this study provide a possible new strategy to induce viral E6 and E7 instability by using HSP90 and GRP78 inhibitors for the treatment of cervical cancers. It has been known that overexpressed HSP90 in tumor cells promotes the stability of many oncoproteins, such as Her-2, Akt, Raf-1, Cdk4, Cdk6, and Src (27). Small-molecule inhibitors that block the activity of HSP90 ATPase, which is essential for the function of HSP90, are currently under evaluation in clinical trials for various types of cancer (67–71) but not for cervical cancer. Thus, our observations that HSP90 and GRP78 regulate viral E6 and E7 stability undoubtedly provide a scientific foundation for future treatment of cervical cancer by using chaperone inhibitors.

MATERIALS AND METHODS

Plasmids, oligonucleotide primers, antibodies, and inhibitors. All mammalian expression vectors and oligonucleotide primers used in this report are summarized in Table S3 in the supplemental material. The siRNA duplex of 5' GACGUGAG/UGUGACUCUAUU 3' and 5' UAGA GUCACA/CUCACGUCGUU 3' was used as si-E6^ΔE7 (oMA63). Monoclonal anti-HPV16 E7 (ED17) and anti-β-actin (Ac-15) antibodies and polyclonal anti-HPV18 E6 N-terminal region (N-17) and anti-GRP78 antibodies were purchased from Santa Cruz Biotechnology (Santa Cruz, CA). Anti-pan-HSP90 polyclonal antibody, anti-HSP90α monoclonal antibody (D1A7), anti-HSP90β monoclonal antibody (D3F2), anti-HSP70 monoclonal antibody (D69), and anti-PRMT5 polyclonal antibody were purchased from Cell Signaling Technology (Danvers, MA). Anti-FLAG (M2) monoclonal antibody, anti-β-tubulin monoclonal antibody (Tub2.1), and anti-c-Myc monoclonal antibody (9E10) were purchased from Sigma-Aldrich (St. Louis, MO). Anti-GFP polyclonal antibody, anti-GFP monoclonal antibody (JL-8), and anti-pRB antibody (G3-245) were from BD Biosciences (San Jose, CA, USA). Anti-p53 monoclonal antibody (DO-1) was purchased from Merck KGaA (Darmstadt, Germany). Anti-neomycin phosphotransferase II rabbit polyclonal antibody was from EMD Millipore (Billerica, MA, USA). Anti-HA (3F10) rat and (HA-7) mouse monoclonal antibodies were purchased from Roche Diagnostics (Basel, Switzerland) and Sigma-Aldrich, respectively. Anti-HPV16 E6 mouse monoclonal antibodies 6F4 and 3F8 were purchased from Euromedex (Souffelweyersheim, France). 17-AAG (17-N-allylamino-17-demethoxygeldanamycin, tanespimycin) was purchased from Merck KGaA. MG132 and cycloheximide were purchased from Sigma-Aldrich.

***In vitro* splicing and lariat RT-PCR.** *In vitro* transcription and an *in vitro* splicing assay of HPV16 E6E7 pre-mRNA (nt 104 to 881) with a U1 binding site at the 3' end were performed as previously described with modifications (12). Sixty nanograms of pre-mRNA was applied for *in vitro* splicing in the presence of 40% HeLa nuclear extract and 3 mM MgCl₂ at 30°C for the times indicated in Fig. 6B. The RT reaction with SuperScript II (Life Technologies, Carlsbad, CA) and PCR by AmpliTaq (Life Technologies) were performed with primers indicated in Fig. 6A and B for the ethanol-precipitated, *in vitro*-spliced RNA products. The lariat RT-PCR products were then subcloned into the pCR2.1 TOPO vector (Life Technologies) and sequenced. *In vitro* splicing assays were performed on 4.0 ng of ³²P-labeled pre-mRNAs in the presence of 40% HeLa nuclear extract and 3 mM MgCl₂ at 30°C for the times indicated in Fig. 6, followed by separation with 6% polyacrylamide gel with 7.5 M urea and exposure to a PhosphorImager screen. The image was captured using a Molecular Dynamics PhosphorImager Storm 860 and analyzed with ImageQuant software.

TABLE 1 Relative quantification of E6^ΔE7 alternative-splicing products^a

Sample name	Sample type	% retention ^b	% of an E6 splice isoform from:		
			nt 226 to 409	nt 226 to 526	nt 226 to 742
CaSki	Cervical cancer cell line	18.4	73.6	7.6	0.5
SiHa	Cervical cancer cell line	54.3	39.8	5.6	0.3
20861	CIN cell line	13.2	79.9	6.6	0.2
20863	CIN cell line	38.3	56.8	4.6	0.4
T1	Cervical cancer	17.0	40.2	24.4	18.4
T2	Cervical cancer	28.4	57.0	13.7	0.9
T3	Cervical cancer	55.2	37.4	7.1	0.2
T4	Cervical cancer	18.4	53.8	26.9	0.9
T5	Cervical cancer	19.5	45.7	34.6	0.2
T6	Cervical cancer	42.0	45.8	11.6	0.7
T7	Cervical cancer	55.9	33.2	10.4	0.4
T8	Cervical cancer	24.2	29.5	32.8	13.5
T9	Cervical cancer	20.2	62.0	16.3	1.5

^a CIN, cervical intraepithelial neoplasia. All samples were infected with HPV16.

^b Refers to retention of the E6 intron (no splicing for E6 expression).

RT-PCR and TaqMan real-time RT-PCR. RT-PCR was performed as described before (12). Briefly, total RNA was treated with Turbo DNase (Roche), followed by RT with a random hexamer primer and Moloney murine leukemia virus (MuLV) reverse transcriptase (Life Technologies). PCR was subsequently performed with AmpliTaq (Life Technologies). For real-time RT-PCR, a TaqMan probe with 5'-6-carboxyfluorescein (FAM) and 3'-carboxytetramethylrhodamine (TAMRA) and oligonucleotide primers were designed from the conserved sequence regions among HPV16 subtypes (Table S3). Total RNA (400 ng) from cervical cancer cells or tissues was used for each real-time RT-PCR, and relative copy numbers of each splice isoform were determined from the cycle threshold (C_T) value of the isoform RNA against a standard curve created from the corresponding cDNA plasmids.

Transfection and immunoprecipitation. Plasmid transfections (2 μ g for each plasmid) were performed with FuGENE HD transfection reagent (Roche Diagnostics) for CaSki and C33A cells in a 6-cm dish and with lipod293 transfection reagent (version II) (SigmaGen Laboratories, Gaithersburg, MD) for HEK293 and HeLa cells. siRNA (40 nM) was transfected with a LipoJet transfection kit (SigmaGen Laboratories), with a 48-h interval if the second transfections were needed for an efficient knockdown. For human primary keratinocytes, 2 μ g of each plasmid was transfected for 1×10^6 cells with a 4D-Nucleofector system (Lonza Cologne GmbH, Cologne, Germany) according to the nucleofection protocol designed for human keratinocytes. For the immunoprecipitation, cells were collected in RIPA buffer (50 mM Tris-HCl [pH 7.4], 150 mM NaCl, 1 mM EDTA, 0.25% sodium deoxycholate, 0.5% NP-40). Following sonication, the cell lysate was treated with RQ1 DNase (Promega, Fitchburg, WI) and RNase A (Life Technologies) and incubated with antibody-conjugated Sepharose 4B (Sigma-Aldrich) for 1 h at 4°C. Precipitated products were then washed with RIPA buffer and eluted with a 2.5 \times SDS protein gel loading solution containing 10% β -mercaptoethanol for Western blotting.

Cell lines and cervical tissues. CaSki cells and SiHa cells are cervical cancer cell lines with an integrated HPV16 genome (200 to 300 copies/cell and 1 to 2 copies/cell, respectively). HeLa cells are a cervical cancer cell line with an integrated HPV18 genome (10 to 50 copies/cell). W12-derived subclone cell lines, 20861 and 20863 cells, originated from a CIN I lesion and contain an integrated (20861 cells) and episomal (20863 cells) HPV16 genome (72). Primary human foreskin keratinocytes (C-001-5C) were purchased from Life Technologies and grown in the presence of J2 feeder cells (73). HPV-negative cervical cancer cell line C33A (mutant p53, mutant pRB), colon cancer cell line HCT116 (mutant ras, wt p53, wt pRB), and adenoviral E1b55k- and E1A-positive human embryonic kidney cell line HEK293 (wt p53, wt pRB) were also used in this study. Total RNAs from HPV16-positive cervical tissues (samples T1 to T9 in Table 1) and raft cultures with HPV16 or HPV18 infection were the RNAs left over

from our previous studies (47). The mRNA expression profiling derived from 5 normal cervix samples and 40 cervical cancer tissue samples in Fig. 1E were obtained from OncoPrint 3.0 (74). Protein extracts from normal cervix (lanes N₁ and N₂ in Fig. 1F) and HPV16-positive cervical cancer tissues (lanes T₁ to T₅ in Fig. 1F) were purchased from US Biomax (Rockville, MD).

Northern blotting. Northern blotting was performed as previously described (75). Briefly, each 5 μ g of total RNA was separated in 1% agarose gel with 1 \times MOPS (morpholinepropanesulfonic acid) buffer with formaldehyde. Separated RNAs were then capillary transferred onto a nylon membrane and cross-linked by UV. Membranes were then prehybridized and incubated with ³²P-labeled probes overnight at 42°C. The following probes were used: oZMZ220 for the detection of HPV16 E6 and E6*1, oZMZ380 for HPV16 E7 and E6^ΔE7, oZMZ296 for enhanced green fluorescent protein (EGFP), and oZMZ270 for GAPDH (Table S2). After exposure to a PhosphorImager screen, the radioactivity was captured and analyzed as described above.

Cycloheximide treatment. For the cycloheximide-chase study, HEK293 cells at 1.5×10^6 in a 6-cm plate were transfected with 2 μ g of pZMZ70 (GFP-E6) or pZMZ74 (GFP-E7) or with 2 μ g of the pCMV3 \times FLAG14 empty vector or pMA48 (E6^ΔE7-HA) for 16 h. Culture medium was then replaced with cycloheximide (0.1 mg/ml)- or 10 μ M MG132-containing medium for the times indicated in Fig. 4. Cells were then collected in 2.5 \times SDS protein sample buffer containing 10% β -mercaptoethanol for Western blotting.

WST-8 cell proliferation assay. To detect dehydrogenase activities in living cells, a WST-8 cell proliferation assay was performed with cell counting kit 8 from Dojindo Molecular Technologies (Rockville, MD), as described previously (76, 77). Briefly, cells were incubated in culture medium with 10% WST-8 cells for 40 min at 37°C. The cell culture media were then measured in triplicate at 450-nm absorbances, and the cell viability was calculated.

LC-MS/MS analysis. Cell lysates of HEK293 cells transfected with pMA15 (FLAG-E6^ΔE7) or the p3 \times FLAG CMV14 (Sigma) empty vector for 48 h were treated with RQ1 DNase (Promega) and RNase A (Life Technologies) before immunoprecipitation with anti-FLAG beads (Sigma). Immunoprecipitation products were separated in 4% to 20% Tris-glycine gel (Bio-Rad) and silver stained with SilverQuest (Life Technologies). Specific protein bands in IP products of FLAG-E6^ΔE7 pull-down experiments were excised from the gel with silver staining. Following destaining, excised gel fragments were dry frosted and rehydrated with trypsin solution. Trypsin-digested peptides were then purified for LC-MS/MS analysis by a service provider, ProtTech (Phoenixville, PA).

Immunocytochemistry and confocal microscopy. Cells were fixed with 4% PFA in phosphate-buffered saline (PBS), permeabilized by 0.1% Tri-

ton X-100, and incubated with 5% bovine serum albumin (BSA) for nonspecific blocking. Subsequently, cells were incubated with a mouse anti-FLAG (M2) monoclonal antibody, followed by incubation with anti-mouse IgG-Alexa 488 and Hoechst stain. Fluorescent and differential interference contrast (DIC) images were obtained with a Zeiss LSM510 Meta confocal microscope (Carl Zeiss MicroImaging, Inc., Thornwood, NY).

SUPPLEMENTAL MATERIAL

Supplemental material for this article may be found at <http://mbio.asm.org/lookup/suppl/doi:10.1128/mBio.02068-14/-/DCSupplemental>.

Table S1, PDF file, 0.1 MB.
Table S2, PDF file, 0.1 MB.
Table S3, PDF file, 0.1 MB.
Figure S1, TIF file, 2.2 MB.
Figure S2, TIF file, 1.6 MB.
Figure S3, TIF file, 2.8 MB.
Figure S4, TIF file, 0.8 MB.
Figure S5, TIF file, 2.9 MB.
Figure S6, TIF file, 2.9 MB.
Figure S7, TIF file, 1.1 MB.

ACKNOWLEDGMENTS

We thank Craig Meyers of Penn State University for the raft tissues infected with HPV16 and HPV18 and Xing Xie and Yang Li of Zhejiang University for total RNAs extracted from anonymized excess cervical cancer tissues that were no longer needed for diagnostic and clinical purposes. We also thank Jeffrey Strathern of NCI and Yihong Ye of NIDDK for their critical comments in the course of this study.

REFERENCES

- Bernard HU, Burk RD, Chen Z, van Doorslaer K, zur Hausen H, de Villiers EM. 2010. Classification of papillomaviruses (PVs) based on 189 PV types and proposal of taxonomic amendments. *Virology* 401:70–79. <http://dx.doi.org/10.1016/j.viro.2010.02.002>.
- Howley PM, Lowy DR. 2007. Papillomaviruses, p 229970–2354. In Knipe DM, Howley PM, Griffin DE, Lamb RA, Martin MA, Roizman B, Straus SE (ed), *Fields virology*, 5th ed. Lippincott Williams & Wilkins, Philadelphia, PA.
- Walboomers JM, Jacobs MV, Manos MM, Bosch FX, Kummer JA, Shah KV, Snijders PJ, Peto J, Meijer CJ, Muñoz N. 1999. Human papillomavirus is a necessary cause of invasive cervical cancer worldwide. *J Pathol* 189:12–19. [http://dx.doi.org/10.1002/\(SICI\)1096-9896\(199909\)189:1<12::AID-PATH431>3.0.CO;2-F](http://dx.doi.org/10.1002/(SICI)1096-9896(199909)189:1<12::AID-PATH431>3.0.CO;2-F).
- Muñoz N, Bosch FX, de Sanjosé S, Herrero R, Castellsagué X, Shah KV, Snijders PJ, Meijer CJ, International Agency for Research on Cancer Multicenter Cervical Cancer Study Group. 2003. Epidemiologic classification of human papillomavirus types associated with cervical cancer. *N Engl J Med* 348:518–527. <http://dx.doi.org/10.1056/NEJMoa021641>.
- Munoz N, Castellsague X, de Gonzalez AB, Gissmann L. 2006. Chapter 1: HPV in the etiology of human cancer. *Vaccine* 24(Suppl 3):S3/1–S3/10. <http://dx.doi.org/10.1016/j.vaccine.2006.05.115>.
- Dürst M, Gissmann L, Ikenberg H, zur Hausen H. 1983. A papillomavirus DNA from a cervical carcinoma and its prevalence in cancer biopsy samples from different geographic regions. *Proc Natl Acad Sci U S A* 80:3812–3815. <http://dx.doi.org/10.1073/pnas.80.12.3812>.
- Zheng ZM. 2010. Viral oncogenes, noncoding RNAs, and RNA splicing in human tumor viruses. *Int J Biol Sci* 6:730–755. <http://dx.doi.org/10.7150/ijbs.6.730>.
- Narisawa-Saito M, Kiyono T. 2007. Basic mechanisms of high-risk human papillomavirus-induced carcinogenesis: roles of E6 and E7 proteins. *Cancer Sci* 98:1505–1511. <http://dx.doi.org/10.1111/j.1349-7006.2007.00546.x>.
- Niebler M, Qian X, Höfler D, Kogoso V, Kaewprag J, Kaufmann AM, Ly R, Böhmer G, Zawatzky R, Rösl F, Rincon-Orozco B. 2013. Post-translational control of IL-1beta via the human papillomavirus type 16 E6 oncoprotein: a novel mechanism of innate immune escape mediated by the E3-ubiquitin ligase E6-AP and p53. *PLoS Pathog* 9:e1003536. <http://dx.doi.org/10.1371/journal.ppat.1003536>.
- Zheng ZM, Baker CC. 2006. Papillomavirus genome structure, expression, and post-transcriptional regulation. *Front Biosci* 11:2286–2302. <http://dx.doi.org/10.2741/1971>.
- Johansson C, Schwartz S. 2013. Regulation of human papillomavirus gene expression by splicing and polyadenylation. *Nat Rev Microbiol* 11:239–251. <http://dx.doi.org/10.1038/nrmicro2984>.
- Ajiro M, Jia R, Zhang L, Liu X, Zheng ZM. 2012. Intron definition and a branch site adenosine at nt 385 control RNA splicing of HPV16 E6*1 and E7 expression. *PLoS One* 7:e46412. <http://dx.doi.org/10.1371/journal.pone.0046412>.
- Smotkin D, Wettstein FO. 1986. Transcription of human papillomavirus type 16 early genes in a cervical cancer and a cancer-derived cell line and identification of the E7 protein. *Proc Natl Acad Sci U S A* 83:4680–4684. <http://dx.doi.org/10.1073/pnas.83.13.4680>.
- Smotkin D, Prokoph H, Wettstein FO. 1989. Oncogenic and nononcogenic human genital papillomaviruses generate the E7 mRNA by different mechanisms. *J Virol* 63:1441–1447.
- Schneider-Gädick A, Schwarz E. 1986. Different human cervical carcinoma cell lines show similar transcription patterns of human papillomavirus type 18 early genes. *EMBO J* 5:2285–2292.
- Zheng ZM, Tao M, Yamanegi K, Bodaghi S, Xiao W. 2004. Splicing of a cap-proximal human papillomavirus 16 E6E7 intron promotes E7 expression, but can be restrained by distance of the intron from its RNA 5' cap. *J Mol Biol* 337:1091–1108. <http://dx.doi.org/10.1016/j.jmb.2004.02.023>.
- Tang S, Tao M, McCoy JP, Jr, Zheng ZM. 2006. The E7 oncoprotein is translated from spliced E6*1 transcripts in high-risk human papillomavirus type 16- or type 18-positive cervical cancer cell lines via translation reinitiation. *J Virol* 80:4249–4263. <http://dx.doi.org/10.1128/JVI.80.9.4249-4263.2006>.
- Pim D, Massimi P, Banks L. 1997. Alternatively spliced HPV-18 E6* protein inhibits E6 mediated degradation of p53 and suppresses transformed cell growth. *Oncogene* 15:257–264. <http://dx.doi.org/10.1038/sj.onc.1201202>.
- Pim D, Banks L. 1999. HPV-18 E6*1 protein modulates the E6-directed degradation of p53 by binding to full-length HPV-18 E6. *Oncogene* 18:7403–7408. <http://dx.doi.org/10.1038/sj.onc.1203134>.
- Pim D, Tomaic V, Banks L. 2009. The human papillomavirus (HPV) E6* proteins from high-risk, mucosal HPV types can direct degradation of cellular proteins in the absence of full-length E6 protein. *J Virol* 83:9863–9874. <http://dx.doi.org/10.1128/JVI.00539-09>.
- Wanichwatanadecha P, Sirisrimangkorn S, Kaewprag J, Ponglikitmongkol M. 2012. Transactivation activity of human papillomavirus type 16. E6*1 on aldo-keto reductase genes enhances chemoresistance in cervical cancer cells. *J Gen Virol* 93:1081–1092. <http://dx.doi.org/10.1099/vir.0.038265-0>.
- Ordóñez RM, Espinosa AM, Sánchez-González DJ, Armendáriz-Borunda J, Berumen J. 2004. Enhanced oncogenicity of Asian-American human papillomavirus 16 is associated with impaired E2 repression of E6/E7 oncogene transcription. *J Gen Virol* 85:1433–1444. <http://dx.doi.org/10.1099/vir.0.19317-0>.
- Mimnaugh EG, Chavany C, Neckers L. 1996. Polyubiquitination and proteasomal degradation of the p185c-erbB-2 receptor protein-tyrosine kinase induced by geldanamycin. *J Biol Chem* 271:22796–22801. <http://dx.doi.org/10.1074/jbc.271.37.22796>.
- Schulte TW, Blagosklonny MV, Romanova L, Mushinski JF, Monia BP, Johnston JF, Nguyen P, Trepel J, Neckers LM. 1996. Destabilization of Raf-1 by geldanamycin leads to disruption of the Raf-1-MEK-mitogen-activated protein kinase signalling pathway. *Mol Cell Biol* 16:5839–5845.
- Basso AD, Solit DB, Chiosis G, Giri B, Tschlis P, Rosen N. 2002. Akt forms an intracellular complex with heat shock protein 90 (Hsp90) and Cdc37 and is destabilized by inhibitors of Hsp90 function. *J Biol Chem* 277:39858–39866. <http://dx.doi.org/10.1074/jbc.M206322200>.
- Lee AS. 2007. GRP78 induction in cancer: therapeutic and prognostic implications. *Cancer Res* 67:3496–3499. <http://dx.doi.org/10.1158/0008-5472.CAN-07-0325>.
- Whitesell L, Lindquist SL. 2005. HSP90 and the chaperoning of cancer. *Nat Rev Cancer* 5:761–772. <http://dx.doi.org/10.1038/nrc1716>.
- Tao M, Kruhlik M, Xia S, Androphy E, Zheng ZM. 2003. Signals that dictate nuclear localization of human papillomavirus type 16 oncoprotein E6 in living cells. *J Virol* 77:13232–13247. <http://dx.doi.org/10.1128/JVI.77.24.13232-13247.2003>.
- Knapp AA, McManus PM, Bockstall K, Moroianu J. 2009. Identification of the nuclear localization and export signals of high risk HPV16 E7 on-

- coprotein. *Virology* 383:60–68. <http://dx.doi.org/10.1016/j.virol.2008.09.037>.
30. Passinen S, Valkila J, Manninen T, Syvälä H, Ylikomi T. 2001. The C-terminal half of Hsp90 is responsible for its cytoplasmic localization. *Eur J Biochem* 268:5337–5342. <http://dx.doi.org/10.1046/j.0014-2956.2001.02467.x>.
 31. Ni M, Zhou H, Wey S, Baumeister P, Lee AS. 2009. Regulation of PERK signaling and leukemic cell survival by a novel cytosolic isoform of the UPR regulator GRP78/BiP. *PLoS One* 4:e6868. <http://dx.doi.org/10.1371/journal.pone.0006868>.
 32. Ni M, Zhang Y, Lee AS. 2011. Beyond the endoplasmic reticulum: atypical GRP78 in cell viability, signalling and therapeutic targeting. *Biochem J* 434:181–188. <http://dx.doi.org/10.1042/BJ20101569>.
 33. Buchkovich NJ, Maguire TG, Paton AW, Paton JC, Alwine JC. 2009. The endoplasmic reticulum chaperone BiP/GRP78 is important in the structure and function of the human cytomegalovirus assembly compartment. *J Virol* 83:11421–11428. <http://dx.doi.org/10.1128/JVI.00762-09>.
 34. Ansari T, Brimer N, Vande Pol SB. 2012. Peptide interactions stabilize and restructure human papillomavirus type 16 E6 to interact with p53. *J Virol* 86:11386–11391. <http://dx.doi.org/10.1128/JVI.01236-12>.
 35. Zanier K, Charbonnier S, Sidi AO, McEwen AG, Ferrario MG, Poussin-Courmontagne P, Cura V, Brimer N, Babah KO, Ansari T, Muller I, Stote RH, Cavarelli J, Vande Pol S, Travé G. 2013. Structural basis for hijacking of cellular LxxLL motifs by papillomavirus E6 oncoproteins. *Science* 339:694–698. <http://dx.doi.org/10.1126/science.1229934>.
 36. Todorovic B, Massimi P, Hung K, Shaw GS, Banks L, Mymryk JS. 2011. Systematic analysis of the amino acid residues of human papillomavirus type 16 E7 conserved region 3 involved in dimerization and transformation. *J Virol* 85:10048–10057. <http://dx.doi.org/10.1128/JVI.00643-11>.
 37. Clemens KE, Brent R, Gyuris J, Münger K. 1995. Dimerization of the human papillomavirus E7 oncoprotein in vivo. *Virology* 214:289–293. <http://dx.doi.org/10.1006/viro.1995.9926>.
 38. Schneider-Poetsch T, Ju J, Eylar DE, Dang Y, Bhat S, Merrick WC, Green R, Shen B, Liu JO. 2010. Inhibition of eukaryotic translation elongation by cycloheximide and lactimidomycin. *Nat Chem Biol* 6:209–217. <http://dx.doi.org/10.1038/nchembio.304>.
 39. Scheffner M, Werness BA, Huibregtse JM, Levine AJ, Howley PM. 1990. The E6 oncoprotein encoded by human papillomavirus types 16 and 18 promotes the degradation of p53. *Cell* 63:1129–1136. [http://dx.doi.org/10.1016/0092-8674\(90\)90409-8](http://dx.doi.org/10.1016/0092-8674(90)90409-8).
 40. Rosenberger S, De-Castro Arce J, Langbein L, Steenbergen RD, Rösl F. 2010. Alternative splicing of human papillomavirus type-16 E6/E6* early mRNA is coupled to EGF signaling via ERK1/2 activation. *Proc Natl Acad Sci U S A* 107:7006–7011. <http://dx.doi.org/10.1073/pnas.1002620107>.
 41. Scheffner M, Münger K, Byrne JC, Howley PM. 1991. The state of the p53 and retinoblastoma genes in human cervical carcinoma cell lines. *Proc Natl Acad Sci U S A* 88:5523–5527. <http://dx.doi.org/10.1073/pnas.88.13.5523>.
 42. Cartegni L, Chew SL, Krainer AR. 2002. Listening to silence and understanding nonsense: exonic mutations that affect splicing. *Nat Rev Genet* 3:285–298. <http://dx.doi.org/10.1038/nrg775>.
 43. Matlin AJ, Moore MJ. 2007. Spliceosome assembly and composition. *Adv Exp Med Biol* 623:14–35. http://dx.doi.org/10.1007/978-0-387-77374-2_2.
 44. Vogel J, Hess WR, Börner T. 1997. Precise branch point mapping and quantification of splicing intermediates. *Nucleic Acids Res* 25:2030–2031. <http://dx.doi.org/10.1093/nar/25.10.2030>.
 45. Zheng ZM, Reid ES, Baker CC. 2000. Utilization of the bovine papillomavirus type 1 late-stage-specific nucleotide 3605 3' splice site is modulated by a novel exonic bipartite regulator but not by an intronic purine-rich element. *J Virol* 74:10612–10622. <http://dx.doi.org/10.1128/JVI.74.22.10612-10622.2000>.
 46. Li Y, Wang X, Ni T, Wang F, Lu W, Zhu J, Xie X, Zheng ZM. 2013. Human papillomavirus type 58 genome variations and RNA expression in cervical lesions. *J Virol* 87:9313–9322. <http://dx.doi.org/10.1128/JVI.01154-13>.
 47. Wang X, Wang H-K, McCoy JP, Banerjee NS, Rader JS, Broker TR, Meyers C, Chow LT, Zheng ZM. 2009. Oncogenic HPV infection interrupts the expression of tumor-suppressive miR-34a through viral oncoprotein E6. *RNA* 15:637–647. <http://dx.doi.org/10.1261/rna.1442309>.
 48. Taiyab A, Sreedhar AS, Rao ChM. 2009. Hsp90 inhibitors, GA and 17AAG, lead to ER stress-induced apoptosis in rat histiocytoma. *Biochem Pharmacol* 78:142–152. <http://dx.doi.org/10.1016/j.bcp.2009.04.001>.
 49. Gallerne C, Prola A, Lemaire C. 2013. Hsp90 inhibition by PU–H71 induces apoptosis through endoplasmic reticulum stress and mitochondrial pathway in cancer cells and overcomes the resistance conferred by Bcl-2. *Biochim Biophys Acta* 1833:1356–1366. <http://dx.doi.org/10.1016/j.bbamcr.2013.02.014>.
 50. Wandinger SK, Richter K, Buchner J. 2008. The Hsp90 chaperone machinery. *J Biol Chem* 283:18473–18477. <http://dx.doi.org/10.1074/jbc.R800007200>.
 51. Lin BY, Makhov AM, Griffith JD, Broker TR, Chow LT. 2002. Chaperone proteins abrogate inhibition of the human papillomavirus (HPV) E1 replicative helicase by the HPV E2 protein. *Mol Cell Biol* 22:6592–6604. <http://dx.doi.org/10.1128/MCB.22.18.6592-6604.2002>.
 52. Bienkowska-Haba M, Williams C, Kim SM, Garcea RL, Sapp M. 2012. Cyclophilins facilitate dissociation of the human papillomavirus type 16 capsid protein L1 from the L2/DNA complex following virus entry. *J Virol* 86:9875–9887. <http://dx.doi.org/10.1128/JVI.00980-12>.
 53. Song H, Moseley PL, Lowe SL, Ozburn MA. 2010. Inducible heat shock protein 70 enhances HPV31 viral genome replication and virion production during the differentiation-dependent life cycle in human keratinocytes. *Virus Res* 147:113–122. <http://dx.doi.org/10.1016/j.virusres.2009.10.019>.
 54. Omlenschläger O, Seiboth T, Zengerling H, Briese L, Marchanka A, Ramachandran R, Baum M, Korbas M, Meyer-Klaucke W, Dürst M, Görlach M. 2006. Solution structure of the partially folded high-risk human papilloma virus 45 oncoprotein E7. *Oncogene* 25:5953–5959. <http://dx.doi.org/10.1038/sj.onc.1209584>.
 55. Stenlund A, Zabielski J, Ahola H, Moreno-Lopez J, Pettersson U. 1985. Messenger RNAs from the transforming region of bovine papilloma virus type I. *J Mol Biol* 182:541–554. [http://dx.doi.org/10.1016/0022-2836\(85\)90240-2](http://dx.doi.org/10.1016/0022-2836(85)90240-2).
 56. Yang YC, Okayama H, Howley PM. 1985. Bovine papillomavirus contains multiple transforming genes. *Proc Natl Acad Sci U. S. A* 82:1030–1034. <http://dx.doi.org/10.1073/pnas.82.4.1030>.
 57. Rintala MA, Louvanto K, Rantanen V, Grénman SE, Syrjänen KJ, Syrjänen SM. 2012. High-risk human papillomavirus associated with incident cervical intraepithelial neoplasia developing in mothers in the Finnish Family HPV Study cohort. *Scand J Infect Dis* 44:115–125. <http://dx.doi.org/10.3109/00365548.2011.619999>.
 58. Guimera N, Lloveras B, Lindeman J, Alemany L, van de Sandt M, Alejo M, Hernandez-Suarez G, Bravo IG, Molijn A, Jenkins D, Cubilla A, Munoz N, de SS, Bosch FX, Quint W. 2013. The occasional role of low-risk human papillomaviruses 6, 11, 42, 44 and 70 in anogenital carcinoma defined by laser capture microdissection/PCR methodology: results from a global study. *Am J Surg Pathol* 37:1299–1310. <http://dx.doi.org/10.1097/PAS.0b013e31828b6be4>.
 59. Arbyn M, Tommasino M, Depuydt C, Dillner J. 2014. Are twenty human papillomavirus types causing cervical cancer? *J Pathol* 234:431–435. <http://dx.doi.org/10.1002/path.4424>.
 60. Longuet M, Beaudenon S, Orth G. 1996. Two novel genital human papillomavirus (HPV) types, HPV68 and HPV70, related to the potentially oncogenic HPV39. *J Clin Microbiol* 34:738–744.
 61. Halec G, Schmitt M, Dondog B, Sharkhuu E, Wentzensen N, Gheit T, Tommasino M, Kommos F, Bosch FX, Franceschi S, Clifford G, Gissmann L, Pawlita M. 2013. Biological activity of probable/possible high-risk human papillomavirus types in cervical cancer. *Int J Cancer* 132:63–71. <http://dx.doi.org/10.1002/ijc.27605>.
 62. Bagarazzi ML, Yan J, Morrow MP, Shen X, Parker RL, Lee JC, Giffear M, Pankhong P, Khan AS, Broderick KE, Knott C, Lin F, Boyer JD, Draghia-Akli R, White CJ, Kim JJ, Weiner DB, Sardesai NY. 2012. Immunotherapy against HPV16/18 generates potent TH1 and cytotoxic cellular immune responses. *Sci Transl Med* 4:155ra138. <http://dx.doi.org/10.1126/scitranslmed.3004414>.
 63. Kenter GG, Welters MJ, Valentijn AR, Lowik MJ, Berends-van der Meer DM, Vloon AP, Essahsah F, Fathers LM, Offringa R, Drijfhout JW, Wafelman AR, Oostendorp J, Fleuren GJ, van der Burg SH, Melief CJ. 2009. Vaccination against HPV-16 oncoproteins for vulvar intraepithelial neoplasia. *N Engl J Med* 361:1838–1847. <http://dx.doi.org/10.1056/NEJMoa0810097>.
 64. Welters MJ, Kenter GG, Piersma SJ, Vloon AP, Löwik MJ, Berends-van der Meer DM, Drijfhout JW, Valentijn AR, Wafelman AR, Oostendorp J, Fleuren GJ, Offringa R, Melief CJ, van der Burg SH. 2008. Induction of tumor-specific CD4+ and CD8+ T-cell immunity in cervical cancer patients by a human papillomavirus type 16 E6 and E7 long peptides

- vaccine. *Clin Cancer Res* 14:178–187. <http://dx.doi.org/10.1158/1078-0432.CCR-07-1880>.
65. Kaeser MD, Pebernard S, Iggo RD. 2004. Regulation of p53 stability and function in HCT116 colon cancer cells. *J Biol Chem* 279:7598–7605. <http://dx.doi.org/10.1074/jbc.M311732200>.
 66. Tan S, de Vries EG, van der Zee AG, de Jong S. 2012. Anticancer drugs aimed at E6 and E7 activity in HPV-positive cervical cancer. *Curr Cancer Drug Targets* 12:170–184. <http://dx.doi.org/10.2174/156800912799095135>.
 67. Saif MW, Erlichman C, Dragovich T, Mendelson D, Toft D, Burrows F, Storgard C, Von Hoff D. 2013. Open-label, dose-escalation, safety, pharmacokinetic, and pharmacodynamic study of intravenously administered CNF1010 (17-(allylamino)-17-demethoxygeldanamycin [17-AAG]) in patients with solid tumors. *Cancer Chemother Pharmacol* 71:1345–1355. <http://dx.doi.org/10.1007/s00280-013-2134-9>.
 68. Goldman JW, Raju RN, Gordon GA, El-Hariry I, Teofilivici F, Vukovic VM, Bradley R, Karol MD, Chen Y, Guo W, Inoue T, Rosen LS. 2013. A first in human, safety, pharmacokinetics, and clinical activity phase I study of once weekly administration of the Hsp90 inhibitor ganetespib (STA-9090) in patients with solid malignancies. *BMC J Cancer* 13:152. <http://dx.doi.org/10.1186/1471-2407-13-152>.
 69. Dickson MA, Okuno SH, Keohan ML, Maki RG, D'Adamo DR, Akhurst TJ, Antonescu CR, Schwartz GK. 2013. Phase II study of the HSP90-inhibitor BIB021 in gastrointestinal stromal tumors. *Ann Oncol* 24:252–257. <http://dx.doi.org/10.1093/annonc/mds275>.
 70. Reddy N, Voorhees PM, Houk BE, Brega N, Hinson JM, Jr., Jillela A. 2013. Phase I trial of the HSP90 inhibitor PF-04929113 (SNX5422) in adult patients with recurrent, refractory hematologic malignancies. *Clin Lymphoma Myeloma Leuk* 13:385–391. <http://dx.doi.org/10.1016/j.clml.2013.03.010>.
 71. Sang J, Acquaviva J, Friedland JC, Smith DL, Sequeira M, Zhang C, Jiang Q, Xue L, Lovly CM, Jimenez JP, Shaw AT, Doebele RC, He S, Bates RC, Camidge DR, Morris SW, El-Hariry I, Proia DA, Sang J, Acquaviva J, Friedland JC, Smith DL, Sequeira M, Zhang C, Jiang Q, Xue L, Lovly CM, Jimenez JP, Shaw AT, Doebele RC, He S, Bates RC, Camidge DR, Morris SW, El-Hariry I, Proia DA. 2013. Targeted inhibition of the molecular chaperone Hsp90 overcomes ALK inhibitor resistance in non-small cell lung cancer. *Cancer Discov* 3:430–443. <http://dx.doi.org/2159-8290.CD-12-0440>.
 72. Jeon S, Allen-Hoffmann BL, Lambert PF. 1995. Integration of human papillomavirus type 16 into the human genome correlates with a selective growth advantage of cells. *J Virol* 69:2989–2997.
 73. Wang X, Meyers C, Wang HK, Chow LT, Zheng ZM. 2011. Construction of a full transcription map of human papillomavirus type 18 during productive viral infection. *J Virol* 85:8080–8092. <http://dx.doi.org/10.1128/JVI.00670-11>.
 74. Rhodes DR, Kalyana-Sundaram S, Mahavisno V, Varambally R, Yu J, Briggs BB, Barrette TR, Anstet MJ, Kincaid-Beal C, Kulkarni P, Varambally S, Ghosh D, Chinnaiyan AM. 2007. OncoPrint 3.0: genes, pathways, and networks in a collection of 18,000 cancer gene expression profiles. *Neoplasia* 9:166–180. <http://dx.doi.org/10.1593/neo.07112>.
 75. Kang JG, Pripuzova N, Majerciak V, Kruhlik M, Le SY, Zheng ZM. 2011. Kaposi's sarcoma-associated herpesvirus ORF57 promotes escape of viral and human interleukin-6 from microRNA-mediated suppression. *J Virol* 85:2620–2630. <http://dx.doi.org/10.1128/JVI.02144-10>.
 76. Ajiro M, Katagiri T, Ueda K, Nakagawa H, Fukukawa C, Lin ML, Park JH, Nishidate T, Daigo Y, Nakamura Y. 2009. Involvement of RQCD1 overexpression, a novel cancer-testis antigen, in the Akt pathway in breast cancer cells. *Int J Oncol* 35:673–681. http://dx.doi.org/10.3892/ijo_00000379.
 77. Park JH, Nishidate T, Kijima K, Ohashi T, Takegawa K, Fujikane T, Hirata K, Nakamura Y, Katagiri T. 2010. Critical roles of mucin 1 glycosylation by transactivated polypeptide N-acetylgalactosaminyltransferase 6 in mammary carcinogenesis. *Cancer Res* 70:2759–2769. <http://dx.doi.org/10.1158/0008-5472.CAN-09-3911>.
 78. Ristriani T, Fournane S, Orfanoudakis G, Travé G, Masson M. 2009. A single-codon mutation converts HPV16 E6 oncoprotein into a potential tumor suppressor, which induces p53-dependent senescence of HPV-positive HeLa cervical cancer cells. *Oncogene* 28:762–772. <http://dx.doi.org/10.1038/ncr.2008.422>.
 79. Courtéte J, Sibling AP, Zeder-Lutz G, Dalkara D, Oulad-Abdelghani M, Zuber G, Weiss E. 2007. Suppression of cervical carcinoma cell growth by intracytoplasmic codelivery of anti-oncoprotein E6 antibody and small interfering RNA. *Mol Cancer Ther* 6:1728–1735. <http://dx.doi.org/10.1158/1535-7163.MCT-06-0808>.
 80. Lagrange M, Charbonnier S, Orfanoudakis G, Robinson P, Zanier K, Masson M, Lutz Y, Trave G, Weiss E, Deryckere F. 2005. Binding of human papillomavirus 16 E6 to p53 and E6AP is impaired by monoclonal antibodies directed against the second zinc-binding domain of E6. *J Gen Virol* 86:1001–1007. <http://dx.doi.org/10.1099/vir.0.80607-0>.
 81. Smith CW, Porro EB, Patton JG, Nadal-Ginard B. 1989. Scanning from an independently specified branch point defines the 3' splice site of mammalian introns. *Nature* 342:243–247. <http://dx.doi.org/10.1038/342243a0>.